Zeitschrift: Schweizerische mineralogische und petrographische Mitteilungen = Bulletin suisse de minéralogie et pétrographie

Band: 83 (2003)

Heft: 2

Artikel: Geochemistry of metabasalts from ophiolitic and adjacent distal continental margin units : Evidence from the Monte Rosa region (Swiss and Italian Alps)

Autor: Kramer, Julia / Abart, Rainer / Müntener, Othmar

DOI: https://doi.org/10.5169/seals-63146

Schweizerische Mineralogische und Petrographische Mitteilungen 83, 217–240, 2003

Geochemistry of metabasalts from ophiolitic and adjacent distal continental margin units: Evidence from the Monte Rosa region (Swiss and Italian Alps)

Julia Kramer[1], *Rainer Abart*[1], *Othmar Müntener*[2], *Stefan M. Schmid*[1] and *Willem-B. Stern*[1]

Abstract

In this paper we present new whole rock analyses of amphibolites from the ophiolitic and adjacent continental tectonic units in the Monte Rosa region. Mg numbers and Ni contents indicate that these amphibolites were derived from fractionated magmas with compositions ranging from E- to N-MORB. Based on their Ni, Ti, REE and Nb systematics, the metabasalts from the ophiolitic Zermatt-Saas and Antrona units and from the continental units of the Furgg zone and the Portjengrat unit are ascribed to a common origin. They represent a coherent suite ranging from T- to N-MORB. In contrast, amphibolites from the continental Siviez-Mischabel and Monte Rosa nappes were derived from enriched MORB and/or gabbroic precursors, which are not related to the metabasalts from the ophiolites, the Furgg zone or the Portjengrat unit.

The geochemical differences between the basalts of the ophiolitic Zermatt-Saas and Antrona units and the adjacent continental Furgg zone and the Portjengrat unit are very subtle. Most mafic rocks were derived from low to moderate degrees of melting of an N-MORB type mantle source. Some compositional parameters such as $(Ce/Sm)_n$, Zr* and $(Nb/Zr)_n$ indicate a transition from T-MORB compositions in the continental units towards less enriched compositions in the ophiolitic units. Y, Ti, V and Zr concentrations are highly correlated in the metabasalts from the Furgg zone, whereas such inter-element correlations are less well defined in the metabasalts from the ophiolitic units. This renders the previously proposed interpretation of the Furgg zone amphibolites as tectonically incorporated ophiolitic fragments unlikely. Our data rather suggest that the distal continental units (Portjengrat unit and Furgg zone) and the nearby ophiolitic units were intruded by similar magmas. Portjengrat unit and Furgg zone are interpreted as a formerly continuous tectonic unit which, based on structural grounds, represents the ocean-continent transition zone of the Briançonnais to the immediately adjacent oceanic Antrona unit. However, the ambiguity in the paleogeographic provenance of the Antrona unit (Valais vs. Piemont-Liguria ocean) cannot be resolved with the existing geochemical data.

Keywords: Metabasalt, geochemistry, continental crust, Furgg zone, Monte Rosa, Central-Western Alps.

1. Introduction

The Western Alpine Arc is characterized by the occurrence of remnants of different Mesozoic oceanic basins (e.g. Stampfli and Marchant, 1997 and references therein; Schmid and Kissling, 2000). In the Penninic nappe edifice of the Monte Rosa region, the Zermatt-Saas and the Antrona ophiolitic units represent the remnants of oceanic crust. They are sandwiched between several slivers of continental crust, which pertain to the Monte Rosa and Siviez-Mischabel nappes, and to the Portjengrat and Stockhorn units (Escher et al., 1997). The situation is illustrated in a schematic geological sketch map of the Monte Rosa region (Fig. 1) and in a simplified N–S cross-section (Fig. 2).

The paleogeographic relations were obscured in the course of polyphase Tertiary deformation. NW-directed nappe stacking started in Eocene times under eclogite facies conditions (deformation phases D1 and D2). This was immediately followed by exhumation during ongoing crustal shortening. Post-collisional SE-directed folding and oblique thrusting of the entire nappe pile (deformation phases D3 and D4) finally resulted in the complex present-day geometry (Figs. 1 and 2).

The paleotectonic reconstruction of the Monte Rosa region is still under discussion (Escher et al., 1997; Froitzheim, 2001; Keller and Schmid, 2001; Kramer, 2002). Controversies partially arise from the interpretation of mafic dykes and boudins, which occur within continental units and which possibly represent derivatives from former

[1] Department of Earth Sciences, University of Basel, Bernoullistr. 32, CH-4056 Basel. <Julia.Kramer@unibas.ch>
[2] Department of Earth Sciences, University of Neuchâtel, Rue Emile Argand 11, CH-2007 Neuchâtel.

0036-7699/03/0083/217

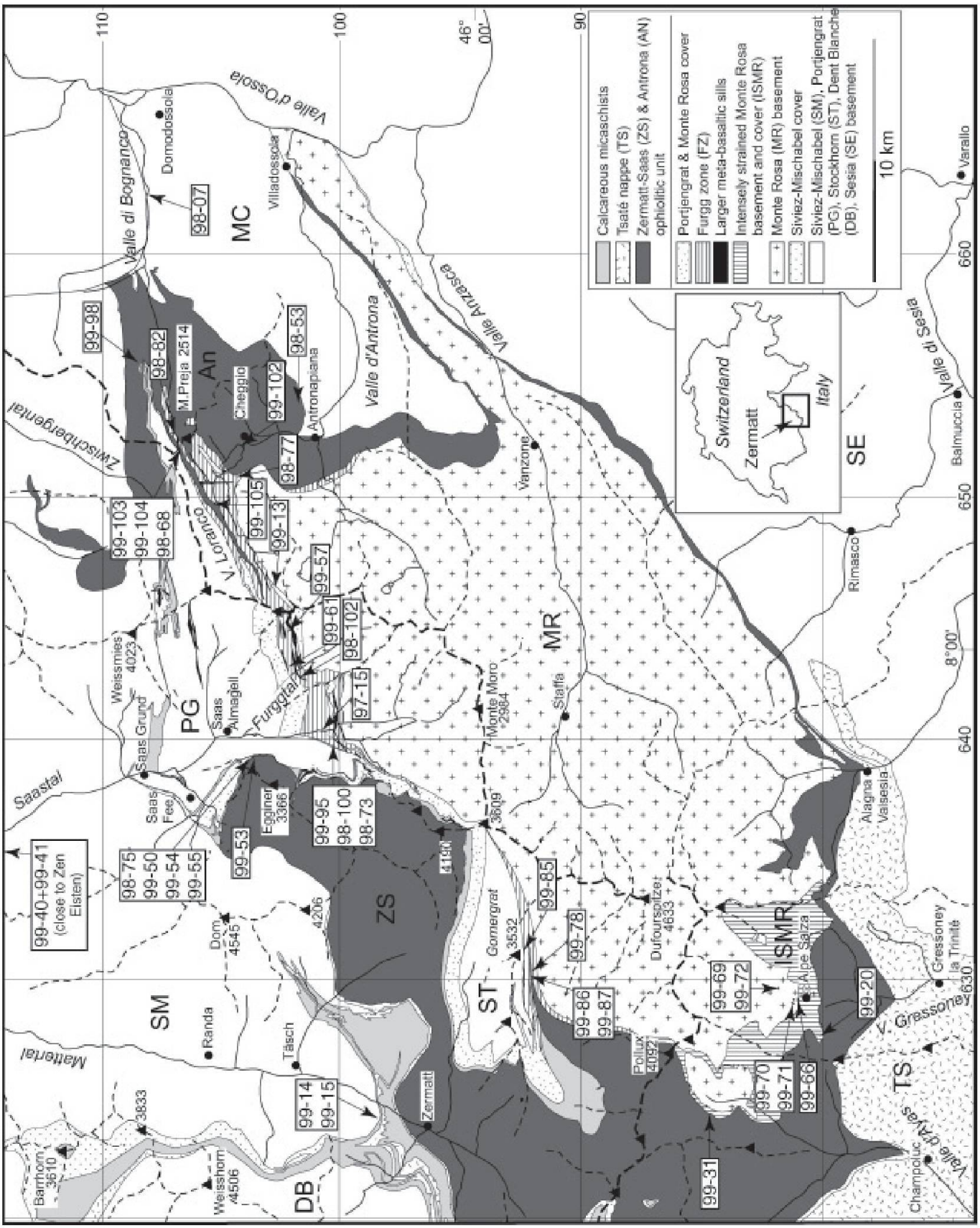

Fig. 1 Sample locations in a simplified geological sketch map of the Monte Rosa region, compiled from Dubach (1998), Keller (2000), Rössler (2000), Weber (2001), Bacher (2002), Bearth (1953a, 1954a,b), Steck et al. (1999), and mapping by Kramer (2002). Swiss kilometric grid is shown.

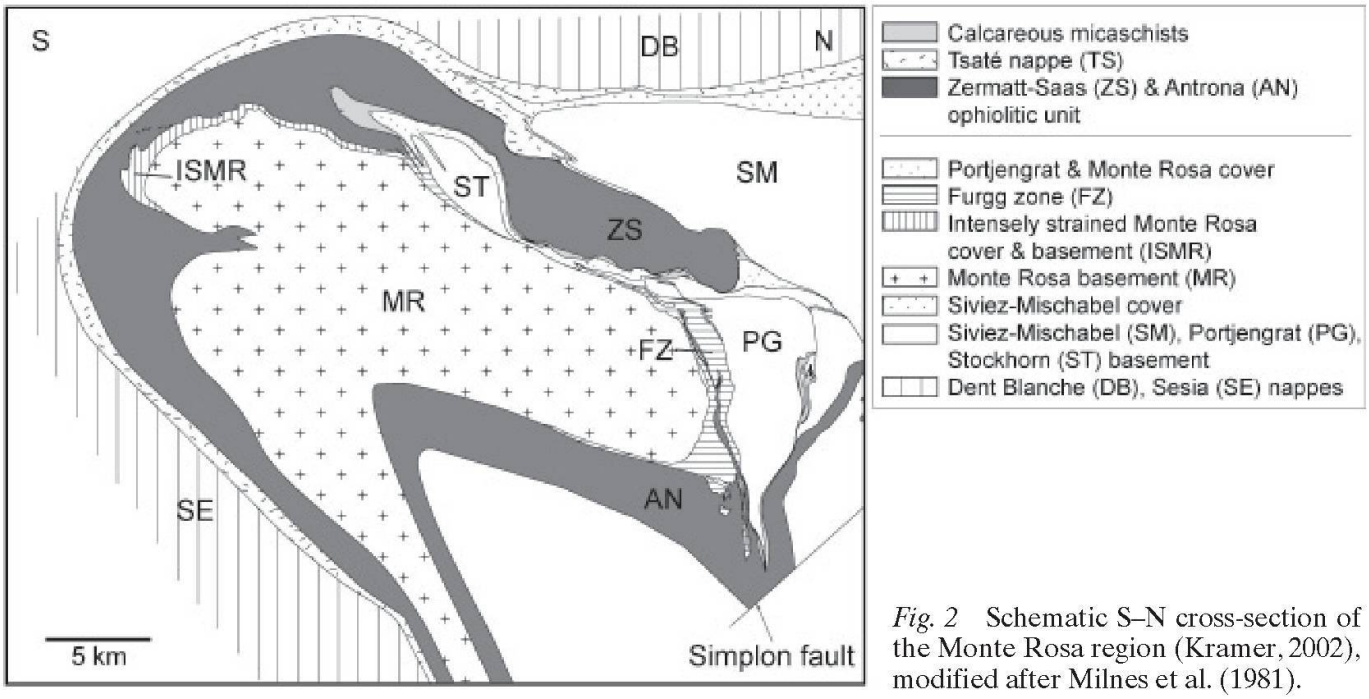

Fig. 2 Schematic S–N cross-section of the Monte Rosa region (Kramer, 2002), modified after Milnes et al. (1981).

oceanic domains. In the Monte Rosa region, mafic dykes and boudins are abundant in both the continental and ophiolitic tectonic units, and they occur in Paleozoic continental crystalline crust, as well as in Mesozoic cover sequences. Mafic boudins are particularly abundant in two mylonitic shear zones that overprint the nappe contacts between continental and ophiolitic tectonic units: (1) in the so-called "Furgg zone" and (2) in the "intensely strained Monte Rosa basement and cover" (Figs. 1 and 2; Kramer, 2002). Due to the abundant mafic boudins, Froitzheim (2001) interpreted the Furgg zone as a tectonic mélange with ophiolitic fragments. Other authors, however, considered the mafic boudins as dyke intrusions into continental lithosphere (e.g. Jaboyedoff et al., 1996), and the Furgg zone as an intracontinental shear zone (Escher et al., 1997; Keller and Schmid, 2001; Kramer, 2002).

In this paper we present new whole rock major and trace element data on mafic rocks collected in (1) the Furgg zone, (2) the adjacent continental Portjengrat unit and in the Monte Rosa and Siviez-Mischabel nappes as well as (3) in the ophiolitic Zermatt-Saas and Antrona units. Our own and previously published data (Beccaluva et al., 1984; Pfeifer et al., 1989) shed light on magma sources and evolution, and on the paleogeographic relations among the tectonic units in the Monte Rosa region.

2. Geological setting

The Monte Rosa nappe forms the "backbone" of the Penninic nappe edifice west of the Lepontine dome. It is comprised of large masses of Permian granitoids and orthogneisses, which were derived from granitoid intrusions (Frey et al., 1976). These granitoids were emplaced into pre-Permian, primarily meta-pelitic paragneisses with subordinate mafic rocks (Hunziker, 1970). The present-day geometry of the Monte Rosa nappe is largely controlled by a large-scale SSE-facing D4 fold, referred to as "Vanzone backfold" by Milnes et al. (1981) and Escher et al. (1988, 1997). The ophiolitic Zermatt-Saas and Antrona units form an almost complete envelope around the continental Monte Rosa nappe, except for the area between Gornergrat and Monte della Preja, where only isolated slivers of ophiolites are present (Fig. 1).

The Furgg zone (FZ in Figs. 1 and 2) and the intensely strained Monte Rosa cover and basement (ISMR in Figs. 1 and 2) represent up to one km thick mylonitic shear zones found north and south of the Monte Rosa main crest, respectively. They overprinted basement-cover contacts of the continental tectonic units, as well as nappe contacts between ophiolitic and continental tectonic units during WNW-directed nappe stacking (deformation phases D1 and D2; Kramer, 2002). Mylonitic shearing resulted in the superposition of two phases of isoclinal and/or sheath folding affecting the nappe contacts between Zermatt-Saas unit and Monte Rosa nappe in case of the ISMR, and between Portjengrat and Stockhorn unit, Monte Rosa nappe and Antrona unit in case of the FZ, respectively (see Fig. 2; Kramer, 2002).

Subsequent reactivation of the Furgg zone during syn-D3 and syn-D4 shearing partly led to the imbrication of isoclinal D1 and D2 folds, now forming isolated fold cores that consist of a varie-

ty of rocks of different provenance which are embedded within a highly strained matrix. D3 and D4 deformation also accounted for large-scale SE-directed folding and dextral oblique thrusting (e.g. Keller and Schmid, 2001; Kramer, 2002), in the course of which both the Furgg zone and the intensely strained Monte Rosa cover and basement were tilted into their present-day structural position enveloping the Monte Rosa nappe.

Several larger coherent imbricates of ultramafic and mafic rocks represent mappable units and were therefore not regarded as part of the Furgg zone, but assigned to the Zermatt-Saas (at Gornergrat) and the Antrona units (at Monte della Preja and in Furggtal), respectively. On structural grounds the numerous smaller mafic boudins found in both Furgg zone and intensely strained Monte Rosa basement and cover, however, are considered as intrusions of former dykes and sills into continental lithosphere, that were overprinted by mylontitic shearing later. Hence, these mafic boudins are regarded as part of both shear zones (FZ and ISMR) overprinting continental tectonic units. It is one of the aims of this publication to test this structural interpretation by adding geochemical data. Note that our structural interpretation differs from the view of Froitzheim (2001), who considers both the large imbricates of ultramafics and the small mafic boudins as ophiolitic imbricates and defines the Furgg zone as an ophiolitic subduction mélange (Froitzheim, 2001).

The intensely strained Monte Rosa cover and basement on the southern side of the Monte Rosa massif (ISMR) was, however, not reactivated during D3 and D4 shearing. There, syn-D1- and D2-shearing mainly resulted in a complex superposition of two mylonitic folding phases on basement and cover of the Monte Rosa nappe. Because of the abundant occurrence of mafic boudins in a highly strained matrix, the ISMR strongly resembles the Furgg zone in the field. However, the two shear zones differ in respect to their tectonic significance, and, as will be shown, also geochemically. Therefore, we distinguish between these two shear zones, although some authors consider the ISMR as part of the FZ (Dal Piaz, 1964; Froitzheim, 2001). In the following we will treat the ISMR as part of the Monte Rosa nappe.

The Portjengrat unit, as well as its southern equivalent, the Stockhorn unit, consists of continental basement and a cover series interpreted to represent Permo-Triassic sediments. The Portjengrat unit is either interpreted as part of the Grand St. Bernhard nappe system (e.g. Bearth, 1956) or as a derivative of the Monte Rosa nappe (e.g. Bearth, 1957; Keller and Schmid, 2001). The Siviez-Mischabel nappe forms the central part of the Grand St. Bernhard nappe system. Whereas its cover comprises only Permo-Triassic rocks in most parts of the region, a complete sedimentary sequence of up to Eocene age is preserved in the "Barrhorn series" in Mattertal (Sartori, 1987, 1990). Since the mafic rocks that were analyzed in this study were sampled in the Furgg zone, the ophiolitic Zermatt-Saas and Antrona units, the continental Monte Rosa and Siviez-Mischabel nappes, as well as in the continental Portjengrat unit, these units will be described here in more detail.

2.1. Furgg zone

The Furgg zone comprises the following rock types derived from the neighbouring tectonic units (Monte Rosa nappe and Portjengrat-Stockhorn unit): para- and orthogneisses of Paleozoic age, along with the adjoining meta-sedimentary cover consisting of garnet micaschists, meta-arkoses, quartzites, and marbles of inferred Permo-Triassic age (Bearth, 1954a,b, 1957; Klein, 1978; Jaboyedoff et al., 1996; Rössler, 2000; Keller and Schmid, 2001; Bacher, 2002; Kramer, 2002). The abundant mafic intercalations, which typically take the form of disrupted layers and boudins are a remarkable feature of the Furgg zone. In some places these mafics represent more than 50% of the rock volume on outcrop scale. In some of the mafic boudins, eclogitic assemblages are preserved (Wetzel, 1972; Liati et al., 2001). As described in the previous section, several larger coherent slivers comprising ultramafics and mafics were mapped as ophiolitic imbricates derived from the Zermatt-Saas or the Antrona ophiolitic unit, and not as part of the Furgg zone (Keller and Schmid, 2001; Bacher, 2002; Kramer, 2002). Between Gornergrat and Monte della Preja (Fig. 1), the Furgg zone overprints the nappe contacts of the Monte Rosa nappe with the Stockhorn and Portjengrat units, respectively (Bearth, 1953a,b, 1954b, 1957; Escher and Sartori, 1991; Escher et al., 1997).

Within less deformed portions of the Furgg zone rock types with a stratigraphy similar to that of the Permo-Triassic meta-sediments in the adjacent Portjengrat-Stockhorn unit and Monte Rosa nappe were mapped (Jaboyedoff et al., 1996; Keller and Schmid, 2001; Bacher, 2002; Kramer, 2002). Such a stratigraphic sequence is particularly well preserved in the Passo della Preja area (Fig. 1), where Triassic dolomite and calcite marbles are associated with rauhwackes, quartzites, and meta-arkoses. These Triassic marbles were intruded by well preserved mafic dykes (see Fig. 5 in

Jaboyedoff et al., 1996), which were collected for chemical analysis ("F4: Furgg zone marbles" in Table 1).

2.2. Zermatt-Saas ophiolitic unit

The Zermatt-Saas unit largely consists of metamorphosed ultramafic and mafic rocks (Bearth and Stern, 1971, 1979; Pfeifer et al., 1989) with a late Jurassic formation age (166–160 Ma, Gebauer, 1999). The associated meta-sediments are manganese-rich quartzites (meta-radiolarites), marbles and calcareous micaschists ("Bündnerschiefer" or "schistes lustrés"; Bearth, 1976; Bearth and Schwander, 1981) of probably late Jurassic to late Cretaceous age (Marthaler, 1981, 1984). The calcareous micaschists may contain meta-basalt boudins. High-pressure peak metamorphic conditions of 2.6–2.8 GPa and 590–630 °C are recorded by meta-radiolarites (Reinecke, 1991, 1998; van der Klauw et al., 1997) while conditions of 1.75–2.0 GPa and 550–600 °C are reported from the ophiolites (Barnicoat and Fry, 1986). Peak metamorphic conditions were reached during the Middle Eocene, i.e. at 44 Ma (Amato et al., 1999; Rubatto and Gebauer, 1999; Gebauer, 1999) while the retrograde greenschist facies overprint occurred during the early Oligocene (Müller, 1989; Barnicoat et al., 1995; Gebauer, 1999).

2.3. Antrona ophiolitic unit

The Antrona unit consists of metamorphosed ultramafic and mafic rocks and associated marbles and calcareous micaschists (Carrupt and Schlup, 1998; Colombi, 1989; Pfeifer et al., 1989). So far, no radiometric formation ages have been reported for the meta-basic rocks. Recently discovered eclogites (Keller, pers. comm.) probably represent the remnants of a high-pressure metamorphic event. Engi et al. (2001) related the peak metamorphic conditions found within the eastern Monte Rosa nappe to the emplacement of this nappe into the surrounding units at 35–40 Ma ago, hence the high pressure metamorphic peak within the adjacent Antrona unit might fall into the same time span. The Oligocene retrograde greenschist facies overprint as a result of the exhumation of the nappe pile, and a prograde amphibolite facies metamorphic overprint in the area of the Lepontine dome were described by Pfeifer et al. (1989) and by Colombi (1989).

2.4. Monte Rosa nappe

The basement of the Monte Rosa nappe consists of pre-Carboniferous paragneisses and calc-silicate rocks (Bearth, 1952, 1954 a, b, 1957; Dal Piaz, 1966, 1971; Escher et al., 1997), which were intruded by late Carboniferous to Permian granites (310–260 Ma; Hunziker, 1970; Frey and Hunziker, 1976; Engi et al., 2001). Peak metamorphic conditions of 2.3 GPa and 520 °C were inferred from white schists within the Monte Rosa basement (Le Bayon et al., 2001) and dated at 35–40 Ma (Hunziker, 1970; Gebauer, 1999).

Meta-sedimentary strata of inferred Permo-Triassic age are rare, but partly preserved in upper Valle d'Ayas, Valle di Gressoney and Valle di Loranco (Keller, 2000; Kramer, 2002). These meta-sediments consist of garnet micaschists, meta-arkoses and quartzites as well as calcite and dolomite marbles. They contain numerous mafic layers and boudins. These meta-sediments are similar to the Permo-Triassic cover of the Portjengrat unit. Yet, they were interpreted as Paleozoic in age by Dal Piaz (1966, 2001). With respect to their spectrum of rock types, boudin-rich parts of the Monte Rosa basement and its meta-sedimentary cover are rather similar to the Furgg zone and referred to as "intensely strained Monte Rosa cover and basement" (ISMR) in Fig. 1.

2.5. Siviez-Mischabel nappe

The Siviez-Mischabel nappe consists of a Paleozoic polymetamorphic basement (Bearth, 1945; Thélin et al., 1993; Escher et al., 1997) and its relatively well-preserved Permo-Mesozoic cover (i.e. Barrhorn series; Marthaler, 1984; Sartori, 1990). In contrast to all the other tectonic units described in this contribution, no eclogite facies event is documented. Nappe emplacement occurred under greenschist facies conditions, estimated at 350 °C to 450 °C and 0.4–0.6 GPa by Sartori (1990) in late Eocene times (Markley et al., 1998). The basement rocks contain numerous mafic layers and boudins (see Thélin et al., 1990; Eisele et al., 1997).

2.6. Portjengrat and Stockhorn units

The Portjengrat unit comprises basement of Paleozoic age, consisting of calc-silicates, paragneisses and orthogneisses (Huang, 1935a,b; Bearth, 1945; Escher et al., 1997) and a cover of presumed Permo-Mesozoic age (Dubach, 1998). Both basement and Permo-Triassic cover contain numerous mafic layers and boudins. In Valle di Loranco, the abundance of mafic layers and boudins, as well as strain intensity, gradually increase towards the Furgg zone (Keller and Schmid, 2001). This is one of the reasons, why we regard the Furgg zone as a shear zone that overprints continental crust, in this case the Portjengrat unit

Table 1 Sample descriptions of the studied amphibolites. For locations see Figure 1.

Sample	Petrography of meta-basaltic sample	Host rock	Swiss coordinates	Location
F1: Boudins, Furgg zone Gornergrat				
99-78	Very fine-grained symplectite of Ab + Act; late stage large poikiloblastic, hypidio- to idiomorphic Zo/ Czo/ Ep; Rt and Ilm rimmed by Ttn; Chl; Bt; poikiloblastic Ab	Garnet mica schists	630 425/ 92 025	Mattertal, Gornergrat, below Stockknubel
99-85	Hypidio- to idiomorphic Act defining mineral lineation; Rt rimmed by Ttn; Fe-bearing carbonate; eye-shaped, deformed Zo/ Czo; Bt from Act; Chl	Dolomitic marbles	631 250/ 92 300	Mattertal, Gornergrat, east of P. 3223
99-86	Idiomorphic, poikiloblastic Grt randomly retrogressed to yellow-green Hbl and symplectite from Ab + yellow-green Act; large grains of Czo/ Zo growing on expense of symplectite; Ilm rimmed by Rt rimmed by Ttn; large grains of Ttn; WM rimmed by Czo/ Zo/ Ep; Hem	Quartzites	630 225/ 92 075	Mattertal, Gornergrat, above Stockknubel
99-87	Fine-grained symplectite from Ab + yellow-green Act; large grains of Czo/ Zo growing on expense of symplectite; Ilm rimmed by Rt rimmed by Ttn; large grains of Ttn; WM rimmed by Czo/ Zo/ Ep; Hem	Garnet mica schists	630 225/ 92 075	Mattertal, Gornergrat, above Stockknubel
F2: Boudins, Furgg zone Saastal				
99-95	Hypidiomorphic to xenomorphic, zoned, yellow-green, actinolitic Hbl; poikiloblastic, xenomorphic Ab; Rt with reaction seams of Ttn; Hem, zoned Czo + Ep; Bt; Chl	Meta- arkoses	639 725/ 100 250	Saastal, below Allalin glacier
98-100	Latest phase: xenomorphic Ab; large zoned, hypidio- to idiomorphic, unaligned Czo; Bt, partly replacing zoned Act (rim Mg-rich, core Fe-rich); Chl growing on expense of Bt; Hem; Ttn	Meta- arkoses	639 825/ 100 225	Saastal, below Allalin glacier
97-15	Latest phase: xenomorphic Ab; zoned, hypidio- to idiomorphic, unaligned Czo; Bt, partly replacing zoned Act (rim Mg-rich, core Fe-rich); Chl growing on expense of Bt; Hem; Rt rimmed by Ttn	Meta- arkoses	640 350/ 100 675	Saastal near Mattmark
98-73	Latest phase: large poikiloblastic, hypidio- to idiomorphic zoned Zo/Czo; fine-grained symplectite from Ab+ Act, Act partly cristallized to larger idiomorphic grains, defining mineral lineation; Bt retrogressed to pale Chl; Ilm rimmed by Rt rimmed by Ttn, Hem; small, poikiloblastic, idiomorphic Grt, large poikiloblastic WM	Garnet mica schists	639 750/ 100 025	Saastal, below Allalin glacier
F3: Boudins, Furgg zone Furggtal & Valle d' Antrona				
98-77	Fine-grained symplectite from Ab+ Act, Act mostly recrystallized to larger hypidiomorphic grains; Ab partly recrystallized to small idiomorphic grains; Bt growing at expense of Act; Rt rimmed by Ttn; Hem	Garnet mica schists	650 825/ 104 275	Valle d' Antrona, W' Lake Bacino dei Cavalli
98-102	Idiomorphic, poikiloblastic Grt randomly retrogressed to blue-green Hbl; blue-green Hbl retrogressed to symplectite from Ab + yellow-green Act; large grains of Czo/ Zo growing on expense of symplectite; Ilm rimmed by Rt rimmed by Ttn; WM; Hem	Garnet mica schists	642 550/ 101 625	SW-side Furggtal
99-57	Fine-grained symplectite of Ab + Act; Act partly recristallizing to larger grains; late stage large poikiloblastic, hypidio- to idiomorphic Zo/ Czo/ Ep; Rt rimmed by Ttn; opaques Ilm?; Chl; Bt	Meta- arkoses	644 450/ 102 075	NE-side Furggtal
99-61	Very fine-grained symplectite from Ab + yellow- green Act; large grains of Czo/ Zo growing on expense of symplectite; Ilm; Rt rimmed by Ttn; WM; Hem	Orthogneisses	642 950/ 102 100	NE-side Furggtal, Augstkummenrinne

Table 1 Continued.

F4: Dykes & sills, Furgg zone marbles, Valle di Loranco & Valle di Bognanco				
98-82	Latest phase: poikiloblastic, hypidio- to idiomorphic zoned Zo/ Czo; fine-grained symplectite from Ab + Act, Act partly recristallized to larger idiomorphic grains, defining mineral lineation; Bt retrogressed to pale Chl; Ilm rimmed by Rt rimmed by Ttn, Hem	Calcitic marbles	652 600/ 106 875	Valle di Bognanco, W' Alpe Preja
98-68	Latest phase: poikiloblastic albitic plagioclase, partly polysynthetic twinned, overgrowing hypidio- and idiomorphic Zo + Czo; Rt rimmed by Ttn; WM; Ank?; hypidiomorphic to idiomorphic, zoned, yellow-green, actinolitic Hbl defining mineral lineation; Hem partly retrogressed to Bt; Bt retrogressed to pale Chl	Calcitic marbles	652 075/ 106 500	Passo della Preja, Valle di Loranco - Valle di Bognanco
99-103	Poikiloblastic albitic plagioclase, overgrowing hypidio- and idiomorphic Zo + Czo; hypidiomorphic to idiomorphic, zoned, yellow-green, actinolitic Hbl; Hem partly retrogressed to Bt; Bt retrogressed to Chl; Rt rimmed by Ttn; WM	Calcitic & dolomitic marbles	652 025/ 106 525	Passo della Preja, Valle di Loranco - Valle di Bognanco
99-104	see 99-103	Calcitic & dolomitic marbles	652 025/ 106 525	Passo della Preja, Valle di Loranco - Valle di Bognanco
O1: Antrona unit				
98-53	Hypidiomorphic to idiomorphic, zoned, yellow-green, actinolitic Hbl defining mineral lineation; polysynthetic twinned Pl + poikiloblastic, xenomorphic, eye-shaped, untwinned Ab with inclusions of Ttn + Ep; zoned Czo + Ep; Rt with reaction seams of Ttn; Hem		653 925/ 101 600	Valle d' Antrona, near Antronapiana
99-98	see above; additionally some Fe-bearing carbonate, late-stage hypidiomorphic Ep/ Czo/ Zo		655 450/ 108 250	Valle di Bognanco, Alpe Vallaro
99-102	Very fine-grained symplectite of Ab + Act; Act partly recristallized to larger grains; late-stage large poikiloblastic, hypidio- to idiomorphic Zo/ Czo/ Ep; Rt and Ilm rimmed by Ttn; very fine-grained cubic opaques Py?; Fe-poor carbonate		652 200/ 104 300	V. d'Antrona, NE-side Lake Bacino dei Cavalli
99-105	see 98-53, additionally large Ep/ Zo/ Czo; Chl	"Loranco amphibolite"	649 725/ 105 200	Valle di Loranco, path to Andolla refuge, near Alpe Campolamana
98-7	Hypidio- to xenomorphic Ep + Czo; Pl, simple and polysynthetic twinned, sericitized; hypidiomorphic to idiomorphic, zoned, yellow-green, actinolitic Hbl defining mineral lineation; hypidio- to xenomorphic Ttn; Chl; late carbonatic sealed cracks	WM-Bt-Qtz-Kfs Orthogneiss	662 500/ 107 900	Valle di Bognanco, 1.5 km E' San Marco, at Simplon shear zone
O2: Zermatt-Saas unit				
99-31	Hypidio- to idiomorphic Act and also Zo/ Czo defining strong mineral lineation; Ab; Ilm rimmed by Rt and Ttn; Rt rimmed by Ttn; WM; Fe-bearing carbonate		624 675/ 84 675	Valle d'Ayas, Mezzalama refuge
99-53	see 99-31, no pronounced mineral lineation, higher amount of idiomorphic Czo/ Zo		639 225/ 103 625	Saastal, path from Plattjen to Britannia refuge
C1: Sills, Siviez-Mischabel basement				
99-14	Poikiloblastic, hypidio- to idiomorphic zoned Zo/ Czo symplectitically intergrown with Ab; fine-grained symplectite from Ab + Act, Act partly cristallized to larger idiomorphic grains; Act retrogressed to Bt; Ttn, Hem	Czo-Ep-Grt-Chl-Bt-WM-Rt-Ilm-Ttn-Apt-Hem-Qtz paragneiss	624 250/ 98 350	Mattertal, NNW' Zermatt, Luegelbach
99-15	see 99-14	Grt-Chl-Bt-WM-Ttn-Apt-Hem-Qtz paragneiss	624 250/ 98 350	Mattertal, NNW' Zermatt, Luegelbach
99-40	see 99-14, no symplectite, but Ab + Act; Ilm rimmed by Ttn	Para- and orthogneiss	635 575/ 115 350	Lower Saastal, near Zen Eisten

Table 1 Continued.

99-41	see 99-14, large amounts of idiomorphic Czo/ Zo/ Ep; Bt retrogressed to Chl	Grt-WM-Chl-Bt-Qtz paragneiss	635 575/ 115 350	Lower Saastal, near Zen Eisten
C2: Boudins, Monte Rosa cover & basement				
99-20	Idiomorphic, poikiloblastic Grt randomly retrogressed to yellow-green Hbl and symplectite from Ab + yellow-green Act; large grains of Czo/ Zo grown on expense of symplectite; Ilm rimmed by Rt rimmed by Ttn; large grains of Ttn; WM rimmed by Czo/ Zo/ Ep; Hem; Qtz	Garnet mica schists; Monte Rosa cover	627 875/ 80 025	Valle di Gressoney, Alpe Bettolina
99-69	Idiomorphic, poikiloblastic Grt randomly retrogressed to blue-green Hbl and partly replaced by Chl + Bt; blue-green Hbl retrogressed to symplectite from Ab + yellow-green Act; poikiloblastic Ab strongly grown on expense of symplectite; Ilm rimmed by Rt rimmed by Ttn; Czo/ Zo; WM; Hem; more intense retrogression than samples above	Meta-arkoses & garnet mica schists; Monte Rosa cover	629 750/ 81 825	Valle di Gressoney, Plateau del Lys
99-70	Poikiloblastic Grt randomly retrogressed to blue-green Hbl and partly replaced by Chl + Bt; blue-green Hbl retrogressed to symplectite from Ab + yellow-green Act; poikiloblastic Ab strongly grown on expense of symplectite; Ilm rimmed by Rt rimmed by Ttn; Czo/ Zo; WM; Hem	WM-Qtz-garnet mica schists; Monte Rosa cover	629 125/ 81 300	Valle di Gressoney, Plateau del Lys
99-71	Yellow-green Act partly symplectitic; poikiloblastic Ab; Rt rimmed by Ttn; Ilm; Hem; Bt; Chl; Fe-poor carbonate	Act-WM-Ab-Grt-Qtz garnet mica schists; Monte Rosa cover	629 125/ 81 300	Valle di Gressoney, Plateau del Lys
99-72	Symplectite of Ab + Act; Act commonly recristallized to larger grains; poikiloblastic Ab; hypidiomorphic Zo/ Czo/ Ep; Rt and Ilm rimmed by Ttn; Chl; Bt	WM-Grt-Act-Chl-Qtz garnet mica schists & meta-arkoses; Monte Rosa cover	629 750/ 81 850	Valle di Gressoney, Plateau del Lys
99-66	Very fine-grained symplectite of Ab + Act; some larger Act; late-stage, large, poikiloblastic, hypidio- to idiomorphic Zo/ Czo/ Ep; Rt rimmed by Ttn	Garnet mica schists, meta-arkoses and orthogneisses; Monte Rosa cover & basement	629 150/ 81 025	Valle di Gressoney, Plateau del Lys
C3: Sills, Portjengrat & Monte Rosa cover				
99-50	Large, poikiloblastic Ab; Ep/ Czo often as inclusions in Ab; Act; Rt rimmed by Ttn; Chl partly intercalated with minor amounts of Bt; Hem; Fe-bearing carbonate	Calcitic & dolomitic marbles; Portjengrat cover	639 200/ 103 725	Saastal, path to Mittaghorn
98-75	Poikiloblastic xenomorphic Ab; mostly small xenomorphic Czo/ Zo/ Ep; Act; Rt rimmed by Ttn; Fe-poor carbonate	Calcitic & dolomitic marbles; Portjengrat cover	639 200/ 104 800	Saastal, path from Plattjen to Britannia refuge
99-55	Act defining mineral lineation; poikiloblastic Ab; hypidio- to idiomorphic Czo/ Ep; Rt rimmed by Ttn; Chl partly intercalated with minor amounts of Bt	Calcitic & dolomitic marbles; Portjengrat cover	639 100/ 103 700	Saastal, below Mittaghorn
99-13	Idiomorphic, poikiloblastic Grt randomly retrogressed to blue-green Hbl; blue-green Hbl retrogressed to symplectite from Ab + yellow-green Act; large grains of Czo/ Zo grown on expense of symplectite; Ilm rimmed by Rt rimmed by Ttn; WM; Hem	Meta-arkoses; Monte Rosa cover	646 250/ 102 650	Val Loranco, S-side Bottarello glacier
99-54	Idiomorphic, poikiloblastic Grt internally replaced by Ep/Czo and randomly retrogressed to yellow-green Hbl; symplectite from Ab + yellow-green Act; large grains of Czo/ Zo grown on expense of symplectite; Ab recrystallized to larger poikiloblastic grains; Ilm rimmed by Rt rimmed by Ttn; WM; Hem; Chl; stronger retrogressed than 99-13	Meta-arkoses; Portjengrat cover	639 050/ 103 750	Saastal, path to Mittaghorn

(see Kramer, 2002). Note, however, that further west (in Furggtal and Saastal), the basement of the Portjengrat unit contains far fewer mafic dykes and boudins (Rössler, 2000; Weber, 2001; Bacher, 2002).

The cover of the Portjengrat unit, which is well preserved e.g. at the Mittaghorn in Saastal and at the Zwischbergen pass in Almagellertal-Zwischbergental (Huang, 1935a,b; Bearth, 1954b, 1957; Dubach, 1998; Kramer, 2002) consists of a sequence of garnet micaschists, meta-conglomerates, meta-arkoses, quartzites, marbles, and rauhwackes. Boudinaged meta-basalt layers are oriented parallel to the main foliation. As the metasediments of presumed Permo-Triassic age have been continuously traced all the way to Gornergrat in Mattertal, the Portjengrat and Stockhorn units are correlated (Kramer, 2002). Near the Stockhorn at Gornergrat, a prograde eclogite facies mineral assemblage of early Oligocene age (34.9 ± 1.4 Ma) is preserved in Permo-Mesozoic quartzites ("Gornergrat series") for which conditions of P < 1.4–1.5 GPa, T < 500–550 °C were estimated by Rubatto and Gebauer (1999).

3. Sample descriptions

Metabasalts sampled for geochemical analysis were taken from the Furgg zone and all adjacent units described above. Sample localities are shown in Fig. 1 and brief sample descriptions are listed in Table 1. Based on their lithologic-tectonic setting, the metabasalts are divided into 9 classes. These classes may be grouped into three broad categories: (1) metabasalts from ophiolitic units (Antrona and Zermatt-Saas units); (2) mafic sills, dykes and boudins, found within continental basement and associated meta-sedimentary cover series (Siviez-Mischabel nappe, Portjengrat-Stockhorn unit and Monte Rosa nappe); (3) metabasalts from the Furgg zone.

3.1. Metabasalts from the Antrona ophiolitic unit (O1)

Three samples were taken from the main body of the Antrona unit (sample 99-98 near Alpe Varallo in Valle di Bognanco; sample 99-102 at Cavalli lake in Valle d'Antrona), one of them close to the contact with the Moncucco-Camughera unit (sample 98-53; Antronapiana in Valle d'Antrona). A large coherent imbricate of the Antrona unit, situated near the Simplon shear zone, was sampled at San Marco in Valle d'Antrona (sample 98-07). The "Loranco-Lappen" (Bearth, 1954 b, 1957) was sampled close to Alpe Campolamana in Valle di Loranco (sample 99-105). Here the Antrona ophiolites occur within the core of an isoclinal antiform (Kramer, 2002), which refolds a mappable tectonic contact between Antrona unit and Furgg zone (Keller, 2000; Bacher, 2002).

3.2. Metabasalts from the Zermatt-Saas ophiolitic unit (O2)

The Zermatt-Saas unit was sampled close to the contact with the Portjengrat-Stockhorn unit (sample 99-53 from Mittaghorn in Saastal) and with the Monte Rosa nappe (sample 99-31 from Mezzalama refuge in Valle d'Ayas), respectively. Sample 99-53 is from the northern limb of the D3 Mittaghorn synform, 50 m south of the contact with the calcareous micaschists. Sample 99-31 was collected ten meters west of the contact with the highly strained sedimentary cover of the Monte Rosa nappe.

3.3. Meta-basalt sills from the continental basement of the Siviez-Mischabel nappe (C1)

Samples were taken at localities in Mattertal and Saastal. The sampling sites are structurally located in the core of the D3 "Mischabel backfold", a south-facing kilometer-scale antiform. Samples 99-14 and 99-15 (near Zermatt in Mattertal) were collected approximately 60 m north of the basement-cover contact. Samples 99-40 and 99-41 (near Zen Eisten in Saastal) were collected within basement far off any tectonic or sedimentary contact. All samples are from up to 1.5 m thick, partly boudinaged and/or isoclinally folded foliation-parallel layers. They are interpreted as early (pre-Alpine?) sills, which intruded the paragneisses of the Siviez-Mischabel nappe and were boudinaged and folded during subsequent deformation.

3.4. Isolated meta-basalt boudins from basement and cover of the southwestern Monte Rosa nappe (C2)

This group comprises samples from the intensely strained Monte Rosa cover and basement in the southwestern part of the Monte Rosa massif (ISMR), which was considered as part of the Furgg zone by some authors (i.e. Dal Piaz, 1964; Froitzheim, 2001). Meta-basalt boudins frequently occur in paragneisses whereas they are scarce in meta-granites. Since one of the metabasalt boudins was found to be intruded by a granite of supposed late Paleozoic age (Kramer, 2002) near the Mezzalama refuge in upper Valle d'Ayas, at least some of these boudins are probably Paleozoic in age. Furthermore, paragneisses occasionally con-

tain pre-Alpine sillimanite, oriented parallel to the foliation and the principal extension direction of the embedded mafic boudins (Dal Piaz, 1966, 1971). This also suggests a Paleozoic age for these metabasalts. Since mafic boudins are abundant within paragneisses of the Monte Rosa nappe, and particularly so near the tectonic contact with the Zermatt-Saas unit, field evidence does not allow us to exclude the possibility that they may represent ophiolitic imbricates incorporated during nappe stacking.

Metabasalts from this group were sampled in Valle di Gressoney at the Alpe Bettolina (sample 99-20) and at the Plateau del Lys (samples 99-66, 99-69, 99-70, 99-71, 99-72). The Bettolina sample (99-20) is from a 0.3 m thick boudin, whereas sample 99-69 is from a large imbricate of approximately 25 by 12 meters in size. The other samples were collected from 3 m thick boudins. Except for sample 99-66, all sampled boudins occur in a matrix of garnet micaschists, which are believed to represent Permo-Mesozoic cover. Sample 99-66 occurs in an intensely strained matrix of isoclinally folded orthogneisses, garnet micaschists and meta-arkoses. As the sample localities are structurally situated in the flat hinge region of the D4 Vanzone antiform, the distance to the nappe contact of the overlying Zermatt-Saas unit, as inferred from cross-section (Kramer, 2002), is probably less than 100 meters. Hence the boudins could also represent tectonically incorporated ophiolitic imbricates.

3.5. Meta-basalt sills from the Permo-Triassic cover of the Portjengrat-Stockhorn unit and northern Monte Rosa nappe (C3)

This group of samples comprises meta-basalt occurrences, which represent intrusions into Permo-Triassic country rocks, for which mélange formation can be excluded. Metabasalts taken from the cover of the Portjengrat-Stockhorn unit were sampled in tectonically relatively undisturbed meta-arkoses and marbles below the Mittaghorn in Saastal (samples 98-75, 99-50, 99-54, 99-55). The samples were collected from 0.6 to 1 m thick, part-

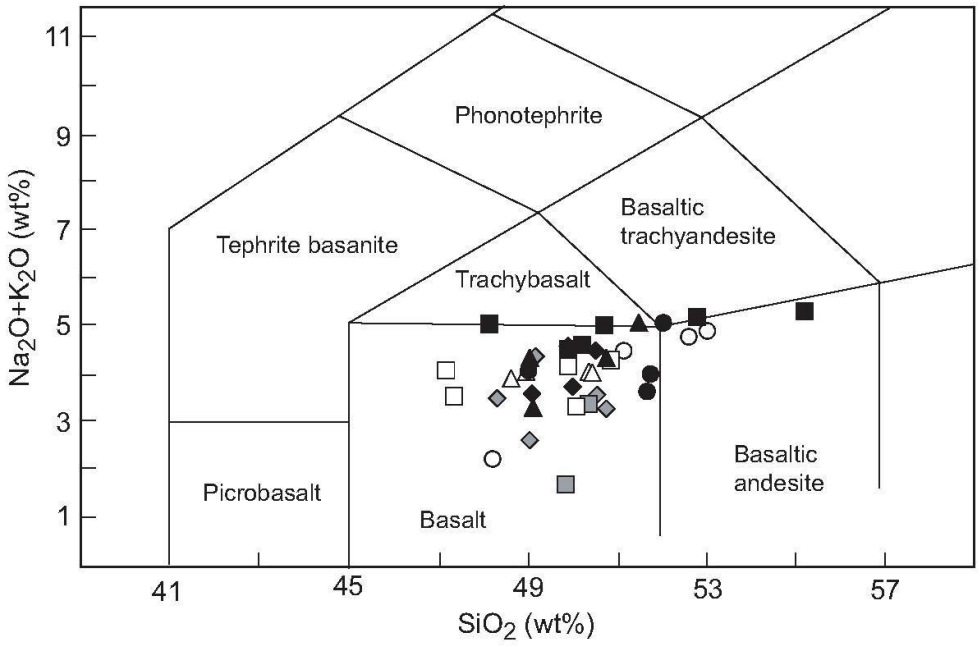

● F1: Boudins from the Furgg zone at Gornergrat
▲ F2: Boudins from the Furgg zone in Saastal
◆ F3: Boudins from the Furggtal and Valle d'Antrona
△ F4: Dykes and sills in marbles of the Furgg zone

◇ O1: Meta-basalts from the Antrona unit
□ O2: Meta-basalts from the Zermatt-Saas unit

○ C1: Sills in basement of the Siviez-Mischabel nappe
■ C2: Boudins from the intensely strained Monte Rosa cover & basement
□ C3: Sills in marbles of the Monte Rosa and Portjengrat cover series

Fig. 3 Total alkali versus silica diagram after Le Bas et al. (1986). The symbols are generally larger than the 3 sigma error.

ly boudinaged foliation-parallel layers, interpreted as sills or parallelized dykes.

One amphibolite was collected from the Monte Rosa unit in Valle di Loranco, i.e. from an approximately 3 m thick, boudinaged foliation-parallel layer, found in carbonate-bearing meta-arkoses of inferred Permo-Triassic age (sample 99-13 at Bottarello glacier).

3.6. Metabasalts from the Furgg zone at Gornergrat (F1)

Here the Furgg zone consists of an association of paragneisses and calc-silicates of supposed Paleozoic age and a cover sequence, including garnet micaschists, meta-arkoses, quartzites and calcite-dolomite marbles of inferred Permo-Triassic age. The meta-basalt samples from this part of the Furgg zone were collected in the Stockchnubel area (samples 99-78, 99-86, 99-87) and east of P. 3223 (sample 99-85; see Table 1 for exact location). Sample 99-78 was collected from an approximately 30 by 10 m large boudin, while the other samples are from smaller boudins up to 1 m in thickness. The boudins in the vicinity of the Stockchnubel are embedded in a matrix of garnet micaschists and quartzites; the sample east of P. 3223 (sample 99-85) is surrounded by a matrix of dolomite marble.

3.7. Metabasalts from the Furgg zone in Saastal (F2)

Here the Furgg zone consists of an assemblage of highly strained, fine-grained orthogneisses and the presumed Permo-Triassic cover of garnet micaschists and subordinate meta-arkoses (see Bearth, 1954b, 1957; Rössler, 2000; Weber, 2001). It contains metabasalts, which were sampled near the Allalin glacier (samples 98-73, 98-100, 99-95) and at the river Saaser Vispa (sample 97-15). Samples from the Allalin glacier area were collected from two up to 0.5 m thick boudins (samples 98-73 and 98-100) and one 3 m thick boudin (sample 99-95), all embedded in garnet micaschists and meta-arkoses. Sample 97-15 (river Saaser Vispa) was collected from a 0.8 m thick boudinaged layer embedded in meta-arkoses.

3.8. Metabasalts from the Furgg zone in Furggtal and in Valle d'Antrona (F3)

Here the Furgg zone mostly comprises the same lithologies as described for Saastal. However, in Valle d'Antrona quartzites occur less and marbles more frequently in the Furgg zone. Mafic boudins are particularly abundant, and some of them are several tens of meters long.

Metabasalts from Furggtal were collected from up to 1.5 m thick boudins embedded in a matrix of meta-arkoses (sample 99-57), garnet micaschists (sample 98-102) and orthogneisses (sample 99-61). The meta-arkoses are intercalated with garnet micaschists, at least partly due to isoclinal folding. One meta-basalt sample collected from Valle d'Antrona (sample 98-77 from west of Lake Cavalli) is from a 1 m thick boudin in a matrix of garnet micaschists. It was collected 100 m east of and structurally below the contact to the basement of the Monte Rosa nappe.

3.9. Dykes and sills in marbles of the Furgg zone (F4)

This group of Furgg zone samples comprises metabasalts found in marbles of the Furgg zone in the Monte della Preja area. Samples are from Alpe Preja (sample 98-82) and from the core of a synform at the Passo della Preja between Valle di Loranco and Valle di Bognanco (samples 98-68, 99-103, 99-104). Here the metabasalts may readily be interpreted as representing sills or parallelized dykes, which intruded Triassic marbles.

The post-Triassic intrusion age is particularly evident for sample 99-104, which was collected from a 0.3 m thick discordant dyke described by Jaboyedoff et al. (1996, see there Fig. 5), obviously post-dating the Triassic marbles. Samples 98-82 and 98-68 were collected from 0.8–1.5 m thick foliation-parallel boudins, sample 99-103 from a 0.6 m thick foliation-parallel layer.

4. Mineralogical composition of metabasalts

All samples are fine-grained, foliated amphibolites, with a grain size of generally less than 2 mm. Mineral parageneses (see Table 1) include yellow and green actinolitic hornblende (act), albitic plagioclase (ab), clinozoisite (cz), zoisite (zo), epidote (ep), chlorite (chl), white mica (wm) and titanite (ttn) +/– biotite (bt). This assemblage is interpreted to have formed during retrograde greenschist facies overprint. Accessory minerals are rutile (rt), ilmenite (ilm), +/– hematite (hem), +/– pyrite (py), +/– zircon (zr), +/– quartz (qtz), +/– calcite (cc).

Relics of an earlier high-pressure metamorphic event could only be identified in amphibolites collected from the Permo-Mesozoic sedimentary cover of the Portjengrat-Stockhorn unit and the Monte Rosa nappe, where abundant garnet is found. This garnet is partly retrogressed to blue-green hornblende and / or chlorite. Wetzel (1972) and Liati et al. (2001) also describe relics of

Table 2 Analytical data, Mg# number, Zr/ Y ratio and Ce_n/Yb_n ratio. For the Ce_n/Yb_n ratio, the Ce and Yb values are chondrite-normalized; normalization values were taken from Boynton (1984).

Tectonic unit	Sample	SiO_2 %	Al_2O_3 %	Fe_2O_3 %	MnO %	MgO %	CaO %	Na_2O %	K_2O %	TiO_2 %	P_2O_5 %	LOI %	Total %	V 51 ppm	Cr 53 ppm	Co 59 ppm	Ni 60 ppm	Cu 63 ppm	Rb 85 ppm	Sr 86 ppm	Y 89 ppm
F1: Boudins, Furgg zone	JK 99-78	51.75	15.61	9.82	0.16	6.57	9.64	3.73	0.31	1.12	0.12	1.03	99.86	252.26	125.47	37.06	18.64	15.55	6.84	238.04	24.24
Gornergrat	JK 99-85	49.00	16.83	9.35	0.15	6.71	8.81	3.80	0.33	1.36	0.22	3.26	99.82	184.34	229.85	38.64	84.72	57.66	9.31	203.23	24.16
	JK 99-86	51.67	16.13	9.46	0.14	6.18	10.24	3.48	0.21	1.48	0.26	0.73	99.96	222.35	254.61	31.18	50.49	32.44	4.60	177.67	27.25
	JK 99-87	52.02	16.06	8.68	0.14	6.48	8.81	4.97	0.16	1.18	0.19	1.22	99.91	182.90	234.22	31.84	79.66	26.03	1.27	179.98	22.16
F2: Boudins, Furgg zone	JK 99-95	50.74	15.24	9.67	0.16	6.34	10.44	3.58	0.82	1.55	0.22	1.11	99.87	235.87	247.21	38.56	44.36	81.08	34.04	260.52	29.18
Saastal	JK 98-100	51.49	15.72	8.38	0.15	6.50	9.99	3.18	1.94	1.27	<0.08	1.24	99.86	190.53	267.42	51.97	66.03	74.13	131.19	141.17	24.23
	JK 97-15	49.02	16.97	9.12	0.15	7.41	10.10	3.19	1.21	1.35	<0.08	1.36	99.87	187.09	208.05	54.09	107.41	38.99	52.78	239.39	25.56
	JK 98-73	49.11	17.11	9.53	0.15	6.99	10.83	3.25	0.11	1.56	<0.08	1.18	99.82	224.00	261.14	48.87	66.84	78.49	1.46	260.21	27.85
F3: Boudins, Furgg zone	JK 98-77	49.09	16.89	9.42	0.16	7.74	10.47	3.08	0.57	1.31	<0.08	1.14	99.87	197.81	257.89	52.38	68.78	54.75	18.84	180.12	23.99
Furggtal & Valle d'Antrona	JK 98-102	49.90	16.35	10.24	0.15	6.95	9.90	4.08	0.55	1.68	<0.08	0.61	100.41	240.98	248.53	52.45	56.08	52.03	24.46	228.25	28.63
	JK 99-57	50.00	16.67	9.27	0.15	6.70	10.52	3.30	0.50	1.45	0.19	1.13	99.88	222.15	251.08	38.47	79.58	87.63	15.02	225.55	28.16
	JK 99-61	50.52	16.06	9.33	0.14	6.32	10.08	4.13	0.40	1.37	0.23	1.07	99.66	214.11	263.43	39.62	64.16	86.74	15.84	202.74	27.10
F4: Dykes & sills, Furgg zone	JK 98-82	48.94	16.67	9.40	0.17	7.09	11.07	3.62	0.49	1.39	<0.08	0.93	99.77	203.82	251.50	56.03	62.20	95.11	12.21	330.30	26.33
marbles, Valle di Loranco &	JK 98-68	48.61	17.18	8.22	0.06	8.58	9.73	3.34	0.62	1.24	<0.08	1.88	99.46	179.32	235.97	49.66	108.84	66.34	23.90	3138.67	22.36
Bognanco	JK 99-103	50.35	16.68	9.20	0.15	6.80	9.99	3.76	0.34	1.42	0.22	0.99	99.90	216.23	250.30	36.98	81.64	85.14	9.60	272.82	27.24
	JK 99-104	50.43	15.81	9.52	0.13	7.49	7.71	3.78	0.29	1.52	0.23	2.77	99.67	238.29	271.61	38.97	54.01	75.38	10.40	1639.41	28.65
O1: Antrona unit	JK 98-53	50.74	16.02	9.30	0.15	6.96	11.29	3.16	0.17	1.35	<0.08	0.68	99.82	236.72	260.49	60.70	96.01	69.04	1.13	167.14	28.64
	JK 99-98	50.54	16.49	8.86	0.13	6.38	10.92	3.46	0.16	1.39	0.24	1.29	99.85	216.93	252.77	37.55	82.76	69.75	1.60	229.81	26.82
	JK 99-102	49.02	15.58	9.43	0.13	4.91	13.90	2.54	0.14	1.57	<0.08	2.75	99.98	253.47	273.17	37.14	98.58	64.75	2.49	140.90	32.95
	JK 99-105	49.15	18.61	8.35	0.11	6.91	8.95	4.15	0.28	1.09	<0.08	2.37	99.97	153.18	208.89	38.51	122.28	97.67	4.27	240.93	20.13
	JK 98-07	48.30	16.21	8.97	0.15	7.54	12.79	2.80	0.74	1.30	<0.08	1.00	99.80	190.46	310.67	50.48	135.55	12.72	17.50	272.44	27.29
O2: Zermatt-Saas unit	JK 99-31	50.35	15.82	9.27	0.16	8.05	9.36	3.09	0.33	1.49	0.21	1.64	99.76	238.78	271.99	37.34	74.10	82.82	3.67	191.22	29.97
	JK 99-53	49.84	14.98	9.48	0.15	7.42	12.70	1.68	0.08	1.34	0.20	1.70	99.55	257.28	360.53	38.30	95.16	19.15	< L.D.	120.96	29.52
C1: Sills, Siviez-Mischabel	JK 99-14	52.60	14.49	10.43	0.15	5.23	7.61	3.67	1.17	1.33	0.26	3.03	99.98	213.99	219.50	33.50	62.64	26.54	43.86	186.40	35.68
basement	JK 99-15	53.03	15.30	10.45	0.15	5.94	7.55	4.26	0.68	1.60	0.25	2.28	101.49	241.67	194.87	35.30	35.40	47.81	18.65	167.19	36.01
	JK 99-40	51.15	14.73	11.45	0.18	6.62	7.31	3.33	1.22	1.64	0.24	2.05	99.91	238.77	102.50	39.47	62.44	10.16	49.83	210.08	29.86
	JK 99-41	48.19	14.44	10.25	0.21	4.06	1.49	1.70	0.58	2.14	1.09	2.21	86.36	278.32	23.63	31.61	10.90	7.40	22.51	695.46	57.91
C2: Boudins, Monte Rosa	JK 99-20	52.80	13.99	11.96	0.15	6.59	6.09	5.01	0.23	1.97	0.42	0.77	99.98	317.48	219.61	43.36	70.30	43.58	2.93	130.20	33.87
cover & basement	JK 99-69	50.21	18.02	10.40	0.14	4.74	9.03	3.59	1.09	1.23	0.19	1.21	99.84	280.19	144.22	34.82	60.75	281.55	48.91	388.82	28.71
	JK 99-70	50.71	15.52	11.29	0.19	5.59	7.48	4.48	0.59	1.85	0.19	1.83	99.71	284.23	194.88	38.30	65.03	21.82	16.31	149.94	41.89
	JK 99-71	48.10	15.29	10.37	0.15	6.74	8.81	3.23	1.87	1.33	0.17	3.73	99.78	196.12	443.48	41.47	131.71	13.30	84.14	146.90	19.03
	JK 99-72	49.90	15.59	10.17	0.18	5.83	10.63	3.05	1.50	1.55	0.26	1.33	99.99	262.33	282.22	30.48	115.10	8.24	62.72	103.33	27.71
	JK 99-66	55.22	14.66	6.80	0.10	6.62	9.38	4.02	1.35	0.45	0.08	1.22	99.89	200.04	463.09	32.74	29.56	<5.00	44.29	34.25	22.59
C3: Sills, Portjengrat &	JK 99-50	47.33	16.89	8.28	0.00	7.97	7.44	3.18	0.40	1.12	0.17	7.08	99.86	171.48	232.90	38.59	109.18	85.51	13.40	186.50	22.05
Monte Rosa cover	JK 98-75	47.14	16.61	8.83	0.14	8.69	7.71	4.03	0.10	1.17	<0.08	5.48	99.90	170.15	242.55	43.01	80.40	65.93	2.27	147.00	22.16
	JK 99-55	49.88	16.62	9.24	0.11	7.36	9.26	3.98	0.23	1.25	0.17	1.77	99.87	197.97	271.66	42.40	73.13	85.11	5.91	197.37	24.65
	JK 99-13	50.86	16.92	8.13	0.13	6.50	10.03	4.26	0.08	0.95	<0.08	2.10	99.97	238.29	103.37	33.52	31.69	13.41	1.68	261.09	21.83
	JK 99-54	50.06	17.24	8.88	0.16	7.42	9.71	3.27	0.11	1.17	0.15	2.04	100.20	231.37	311.26	36.40	104.02	14.06	1.51	165.55	27.15

Table 2 Continued.

Tectonic unit	Sample	Zr 90 ppm	Nb 93 ppm	La 139 ppm	Ce 140 ppm	Pr 141 ppm	Nd 145 ppm	Sm 147 ppm	Eu 151 ppm	Gd 157 ppm	Tb 159 ppm	Dy 161 ppm	Ho 165 ppm	Er 166 ppm	Tm 169 ppm	Yb 174 ppm	Lu 175 ppm	Ta 181 ppm	mg-# value	Zr/Y ratio	Ce_n/Yb_n ratio
F1: Boudins, Furgg zone	JK 99-78	63.00	1.71	4.43	11.09	1.64	8.51	2.92	1.08	3.68	0.56	3.95	0.87	2.35	0.39	2.44	0.39	0.14	57	2.60	1.18
Gornergrat	JK 99-85	110.06	4.54	5.50	15.02	2.08	10.79	2.88	1.11	3.71	0.64	4.14	0.92	2.39	0.40	2.21	0.37	0.36	59	4.55	1.76
	JK 99-86	128.70	5.02	5.55	15.58	2.38	11.41	3.19	1.17	3.81	0.68	4.36	0.94	2.67	0.39	2.64	0.42	0.35	56	4.72	1.53
	JK 99-87	101.25	3.51	4.46	12.66	1.97	10.05	2.90	1.13	3.63	0.60	3.57	0.79	2.17	0.32	2.29	0.38	0.26	60	4.57	1.43
F2: Boudins, Furgg zone	JK 99-95	132.41	4.40	6.08	17.15	2.51	13.60	3.62	1.48	4.66	0.75	4.78	1.01	2.89	0.44	2.82	0.44	0.36	57	4.54	1.58
Saastal	JK 98-100	102.24	4.78	4.10	12.18	1.92	9.23	3.01	1.06	3.74	0.60	3.98	0.81	2.28	0.35	2.24	0.34	0.70	61	4.22	1.41
	JK 97-15	111.75	3.19	4.55	13.49	2.08	11.21	3.25	1.25	3.95	0.65	4.33	0.92	2.53	0.40	2.62	0.40	0.66	62	4.37	1.33
	JK 98-73	126.68	5.13	6.46	17.55	2.58	12.39	3.55	1.34	4.49	0.74	4.41	1.02	2.85	0.41	2.63	0.37	0.69	59	4.55	1.72
F3: Boudins, Furgg zone	JK 98-77	108.80	3.79	4.83	13.97	2.10	9.99	2.98	1.31	3.44	0.64	3.79	0.83	2.33	0.36	2.30	0.34	0.60	62	4.53	1.57
Furggtal & Valle d'Antrona	JK 98-102	137.95	5.84	6.35	17.20	2.51	12.09	3.28	1.24	4.10	0.78	4.60	0.99	2.64	0.42	2.73	0.39	0.84	57	4.82	1.63
	JK 99-57	125.56	4.14	5.49	15.46	2.34	11.92	3.37	1.34	4.47	0.69	4.53	0.91	2.58	0.42	2.64	0.45	0.33	59	4.46	1.51
	JK 99-61	118.68	4.07	5.63	14.87	2.29	11.45	3.45	1.30	4.08	0.71	4.37	0.95	2.51	0.43	2.62	0.43	0.33	57	4.38	1.47
F4: Dykes & sills, Furgg zone	JK 98-82	114.81	3.77	4.96	14.20	2.16	10.77	3.02	1.23	3.80	0.64	4.09	0.91	2.35	0.39	2.41	0.37	0.72	60	4.36	1.53
marbles, Valle di Loranco &	JK 98-68	102.35	3.66	4.94	13.79	2.07	10.43	2.93	1.16	3.42	0.56	3.72	0.79	2.14	0.35	2.15	0.31	0.50	67	4.58	1.66
Bognanco	JK 99-103	125.72	4.09	5.57	16.12	2.35	11.76	3.70	1.38	4.23	0.68	4.51	0.96	2.71	0.41	2.53	0.45	0.33	59	4.62	1.65
	JK 99-104	130.26	4.42	5.85	16.99	2.64	12.88	3.79	1.41	4.72	0.76	5.01	1.01	2.75	0.45	2.72	0.42	0.37	61	4.55	1.61
O1: Antrona unit	JK 98-53	101.08	2.18	3.60	11.25	1.76	10.24	3.12	1.19	3.81	0.68	4.48	0.97	2.56	0.42	2.75	0.42	0.68	60	3.53	1.06
	JK 99-98	119.18	3.45	5.22	14.75	2.30	12.01	3.25	1.26	4.47	0.68	4.14	0.93	2.58	0.39	2.66	0.40	0.29	59	4.44	1.44
	JK 99-102	125.85	2.42	3.91	12.71	2.14	11.20	3.68	1.30	4.62	0.86	5.43	1.08	3.27	0.52	2.96	0.51	0.21	51	3.82	1.11
	JK 99-105	83.95	2.26	3.67	10.45	1.65	8.38	2.39	1.07	2.91	0.52	3.35	0.73	2.07	0.32	1.95	0.30	0.19	62	4.17	1.39
	JK 98-07	85.59	1.56	3.42	10.13	1.74	8.61	2.97	1.18	4.10	0.65	4.46	0.91	2.49	0.40	2.46	0.37	0.38	62	3.14	1.06
O2: Zermatt-Saas unit	JK 99-31	123.37	3.18	4.89	14.59	2.24	11.58	3.41	1.35	4.54	0.79	5.06	1.05	2.92	0.45	3.00	0.46	0.29	63	4.12	1.26
	JK 99-53	100.05	1.86	3.40	11.07	1.79	9.85	3.42	1.31	4.61	0.72	4.63	1.03	2.84	0.46	2.85	0.50	0.17	61	3.39	1.00
C1: Sills, Siviez-Mischabel	JK 99-14	120.36	4.53	9.53	23.92	3.46	16.10	4.60	1.59	5.61	0.95	6.13	1.24	3.57	0.53	3.63	0.54	0.40	50	3.37	1.70
basement	JK 99-15	180.85	4.96	10.95	27.12	3.74	18.43	5.20	1.63	6.01	0.96	6.19	1.27	3.48	0.53	3.84	0.57	0.43	53	5.02	1.83
	JK 99-40	149.31	4.29	9.54	24.17	3.27	15.10	4.30	1.37	5.05	0.80	5.03	1.04	2.86	0.46	2.90	0.48	0.37	53	5.00	2.15
	JK 99-41	203.19	13.15	20.38	48.44	6.58	30.18	8.19	2.91	9.93	1.61	9.69	1.97	5.36	0.74	4.93	0.75	0.87	44	3.51	2.54
C2: Boudins, Monte Rosa	JK 99-20	154.48	9.51	9.68	24.22	3.35	16.11	4.41	1.53	5.58	0.92	5.88	1.25	3.47	0.51	3.47	0.52	0.77	52	4.56	1.81
cover & basement	JK 99-69	85.21	4.24	10.29	24.62	3.43	15.41	4.31	1.93	4.54	0.73	4.67	0.98	2.58	0.45	2.80	0.44	0.26	47	2.97	2.28
	JK 99-70	186.26	7.15	10.54	25.14	3.43	16.54	4.37	1.29	5.47	1.00	6.57	1.45	3.99	0.66	4.53	0.72	0.50	50	4.45	1.44
	JK 99-71	88.50	13.53	8.40	17.81	2.16	9.84	2.54	0.74	3.49	0.55	3.43	0.69	1.69	0.26	1.73	0.26	1.07	56	4.65	2.66
	JK 99-72	118.20	9.45	10.70	25.12	3.50	15.60	4.03	1.36	4.45	0.70	4.55	0.98	2.62	0.44	2.76	0.43	0.69	53	4.27	2.35
	JK 99-66	50.90	2.17	6.73	14.92	1.87	8.04	2.15	0.41	2.64	0.52	3.62	0.76	2.25	0.35	2.27	0.37	0.25	66	2.25	1.70
C3: Sills, Portjengrat &	JK 99-50	92.44	2.41	3.69	11.12	1.73	8.80	2.64	1.14	3.58	0.56	3.79	0.78	2.16	0.34	2.25	0.35	0.20	66	4.19	1.28
Monte Rosa cover	JK 98-75	89.76	2.63	3.74	11.20	1.73	8.21	2.66	1.03	3.28	0.54	3.47	0.79	2.15	0.32	2.09	0.32	0.32	66	4.05	1.38
	JK 99-55	104.15	3.43	4.73	13.21	1.95	10.04	2.88	1.15	3.59	0.64	3.88	0.84	2.48	0.38	2.46	0.39	0.27	61	4.23	1.39
	JK 99-13	50.57	1.46	3.48	9.24	1.40	7.38	2.47	1.09	3.36	0.54	3.60	0.74	2.19	0.32	2.29	0.37	0.13	61	2.32	1.04
	JK 99-54	92.56	1.74	3.42	10.67	1.82	10.05	3.09	1.27	4.33	0.69	4.36	0.93	2.65	0.42	2.62	0.42	0.14	62	3.41	1.05

high-pressure assemblages within amphibolites of the Furgg zone (see below). Two generations of albitic plagioclase and actinolitic hornblende are common. A first generation of plagioclase and hornblende (ab 1, act 1) forms symplectites which partly replace blue-green hornblende and, probably more commonly, former omphacite (see Kramer, 2002). These symplectites are replaced by a second generation of synkinematically grown albite and actinolitic hornblende (ab 2, act 2), or by post-kinematic clinozoisite and zoisite. The retrograde breakdown of garnet produced chlorite, zoisite/ clinozoisite and more rarely blue-green or yellow-green hornblende. Titanite is commonly the breakdown product of ilmenite and rutile, but also occurs as xenoblastic grains in the matrix.

5. Whole rock chemistry

5.1. Analytical methods

Samples were carefully selected to avoid cracks or veins, and weathered crusts were removed. The samples were crushed in a jawbreaker and ground in an agate mill to grain sizes < 60 µm. For major element analyses 300 mg of ignited powder were mixed with 4700 mg of dried $Li_2B_4O_7$ and fused to glass discs. The XRF analyses (SRS-3400 Bruker-AXS) were done at the geochemical laboratory of the University of Basel. The statistical uncertainty at the 3 sigma-level is less than 2 relative % for all major elements, except for K_2O (5–10 relative %) and TiO_2 (2–20 relative %). Trace elements were analyzed by ICP-MS at the CNRS in Nancy, France. For this purpose, 300 mg of sample powder were fused with $LiBO_2$ and dissolved in HNO_3. Detection limits range from 0.01 to 6 ppm (Table 2). Uncertainties are usually less than 10 relative % except for values close to the detection limit.

5.2. Major and trace element composition

The major and trace element compositions of the amphibolites are given in Table 2. Additional analyses from the Zermatt-Saas and Antrona ophiolitic units may be found in Pfeifer et al. (1989). The SiO_2 concentrations generally fall into a range between 46 and 52 wt%. In the total alkali versus silica (TAS) diagram after Le Bas et al. (1986), the analyses plot into the basalt and basaltic andesite fields (Fig. 3). However, all samples are amphibolites and it is therefore likely that alkali metals were affected to some degree by either ocean floor (hydrothermal) and/or regional metamorphism (Pearce, 1976; MacGeehan and

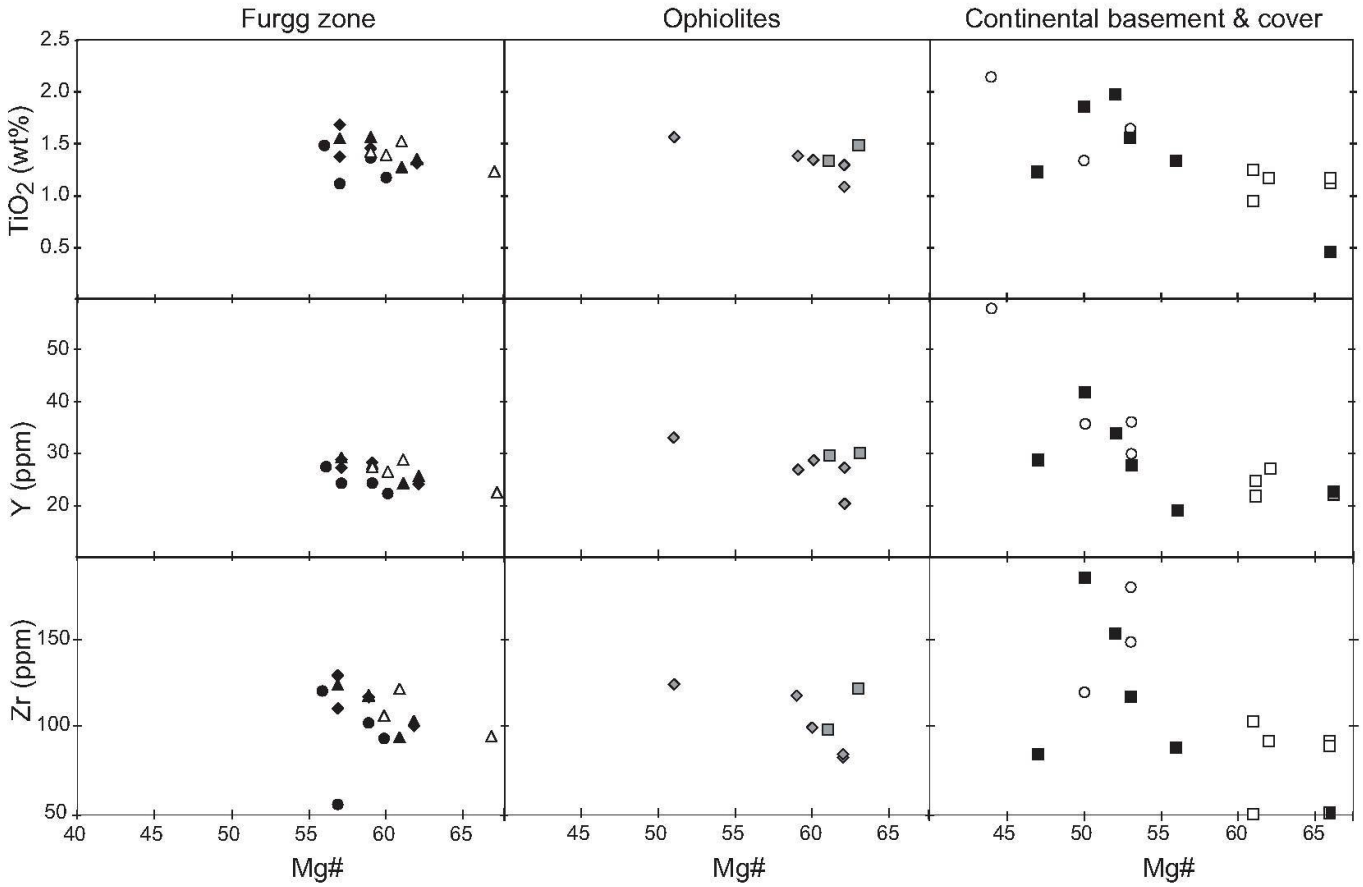

Fig. 4 Concentrations of selected major and trace elements versus Mg# (MgO/(MgO+FeOtot) in moles); symbols as in Fig. 3.

MacLean, 1980; Gelinas et al., 1982; Mottl, 1983; Rollinson, 1983; Saunders and Tearney, 1984). The same is true for other large ion lithophile elements (LILE; Cs, Rb, Ba, Pb and Sr), which is reflected by large concentration variations in the individual samples (see Table 2 and Fig. 7). This makes it difficult to use major elements and especially the alkali metals to decipher the igneous history of the amphibolites. Therefore we mainly rely on trace elements in the following discussion, which are considered to be less mobile during alteration and metamorphism (Dostal and Capedri, 1979; Grauch, 1989; Gelinas et al., 1982; Humphris, 1984).

The large range of MgO (4.06–8.62 wt%) coupled with relatively low Ni contents (< 140 ppm, Table 2, see also Fig. 8) indicates that all amphibolites are derived from differentiated magmas and do not represent unmodified liquids that were in equilibrium with the mantle. This is illustrated in Fig. 4. Mg# (molar $Mg/(Mg+Fe_{tot})$) are less than 65 and decrease with increasing incompatible element contents.

Harker diagrams of selected major and trace elements (Fig. 5) show that incompatible elements (Ti, Y, V) are positively correlated with Zr. These correlations are well defined for the samples from the Furgg zone, but less clear for the

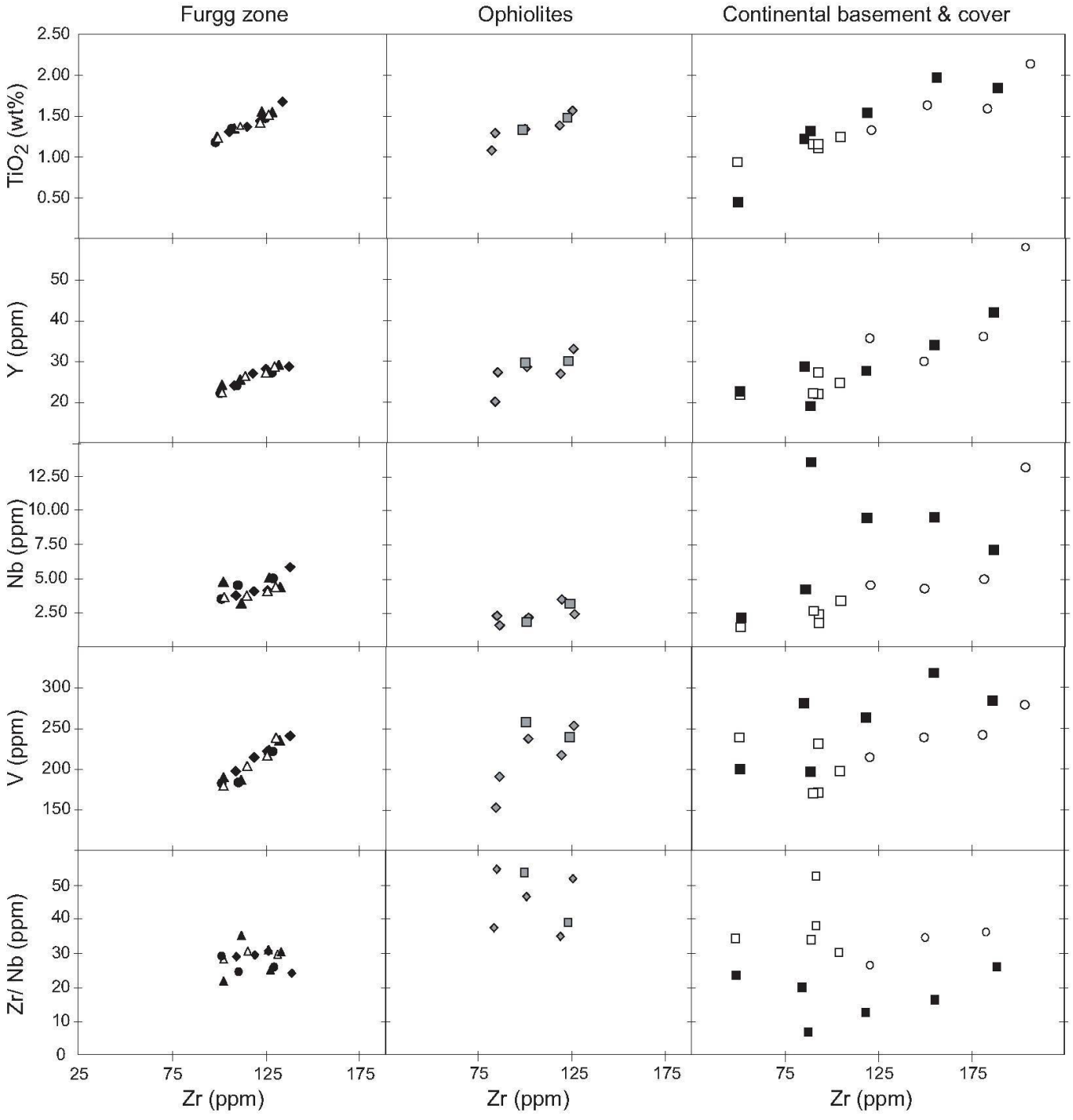

Fig. 5 Concentrations of selected major and trace elements versus Zr concentrations; symbols as in Fig. 3.

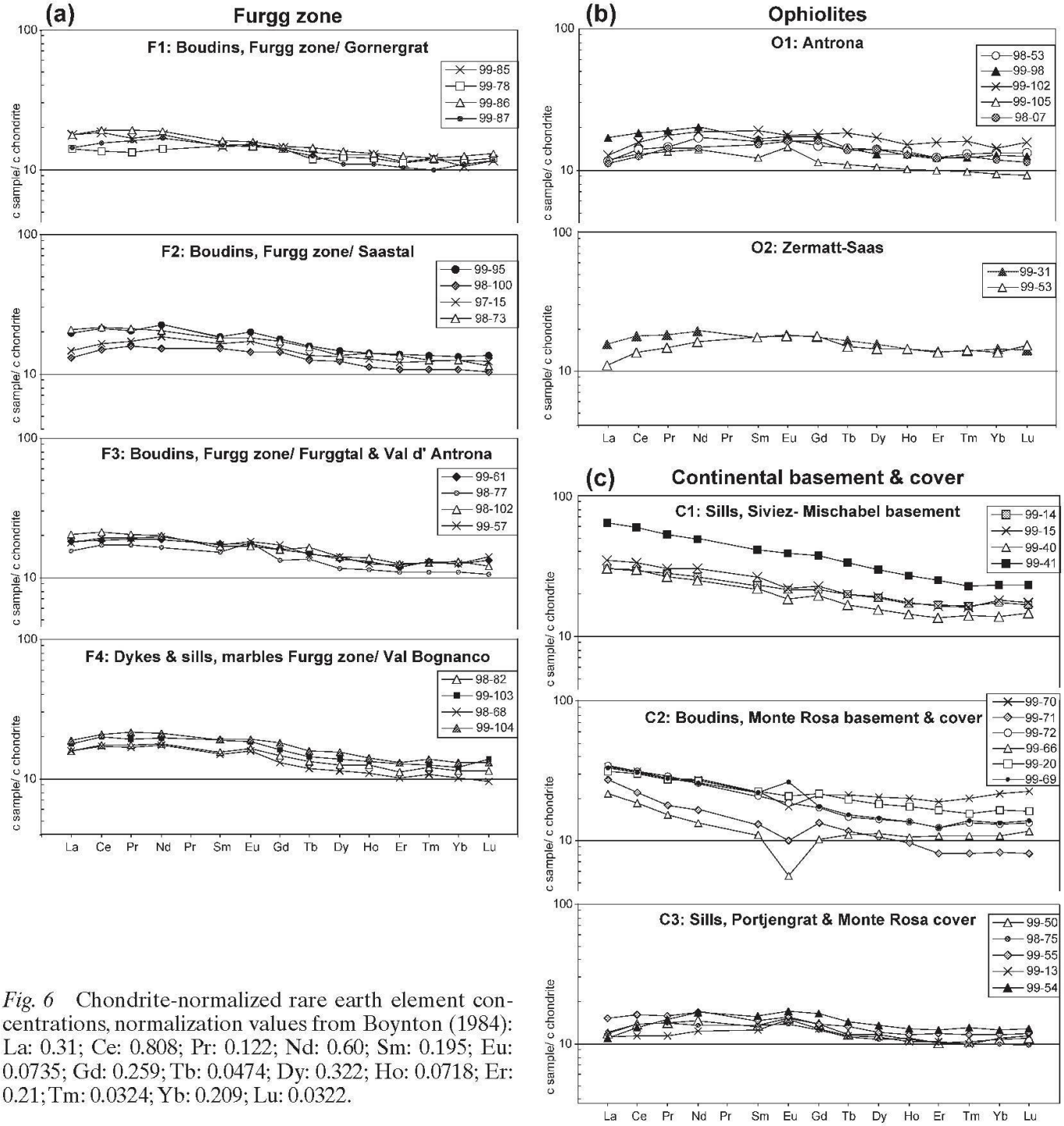

Fig. 6 Chondrite-normalized rare earth element concentrations, normalization values from Boynton (1984): La: 0.31; Ce: 0.808; Pr: 0.122; Nd: 0.60; Sm: 0.195; Eu: 0.0735; Gd: 0.259; Tb: 0.0474; Dy: 0.322; Ho: 0.0718; Er: 0.21; Tm: 0.0324; Yb: 0.209; Lu: 0.0322.

ophiolitic units and the C1 and C2 units. This suggests that the Furgg zone amphibolites were derived form a single cogenetic magma suite, whereas a more heterogeneous magma source and/or a more heterogeneous magma evolution was associated with mafic magmatism in the ophiolitic units.

The Zr/Nb ratio in metabasalts from the ophiolitic units is about 30 (Fig. 5). Samples from the Furgg zone generally plot at somewhat lower Zr/Nb ratios indicating a higher T-type MORB affinity than the classical N-type MORB of the ophiolitic units (Wood et al., 1979).

In MORB the REE concentrations may vary from less than 10 times chondritic in primitive basalts to about 50 times chondritic in more evolved basalts (Schilling et al., 1983; Venturelli et al., 1981; Pearce, 1982; Cullers and Graf, 1984; Henderson, 1984; Saunders, 1984; Rollinson, 1993; Desmurs et al., 2002). Low-pressure fractional crystallization leads to an overall enrichment of the incompatible elements, but does not change the slope of the REE pattern (Schilling, 1983; Frey et al., 1976). This is why the shape of REE patterns observed in evolved basalts largely reflects the REE chemistry of the parent liquid, and

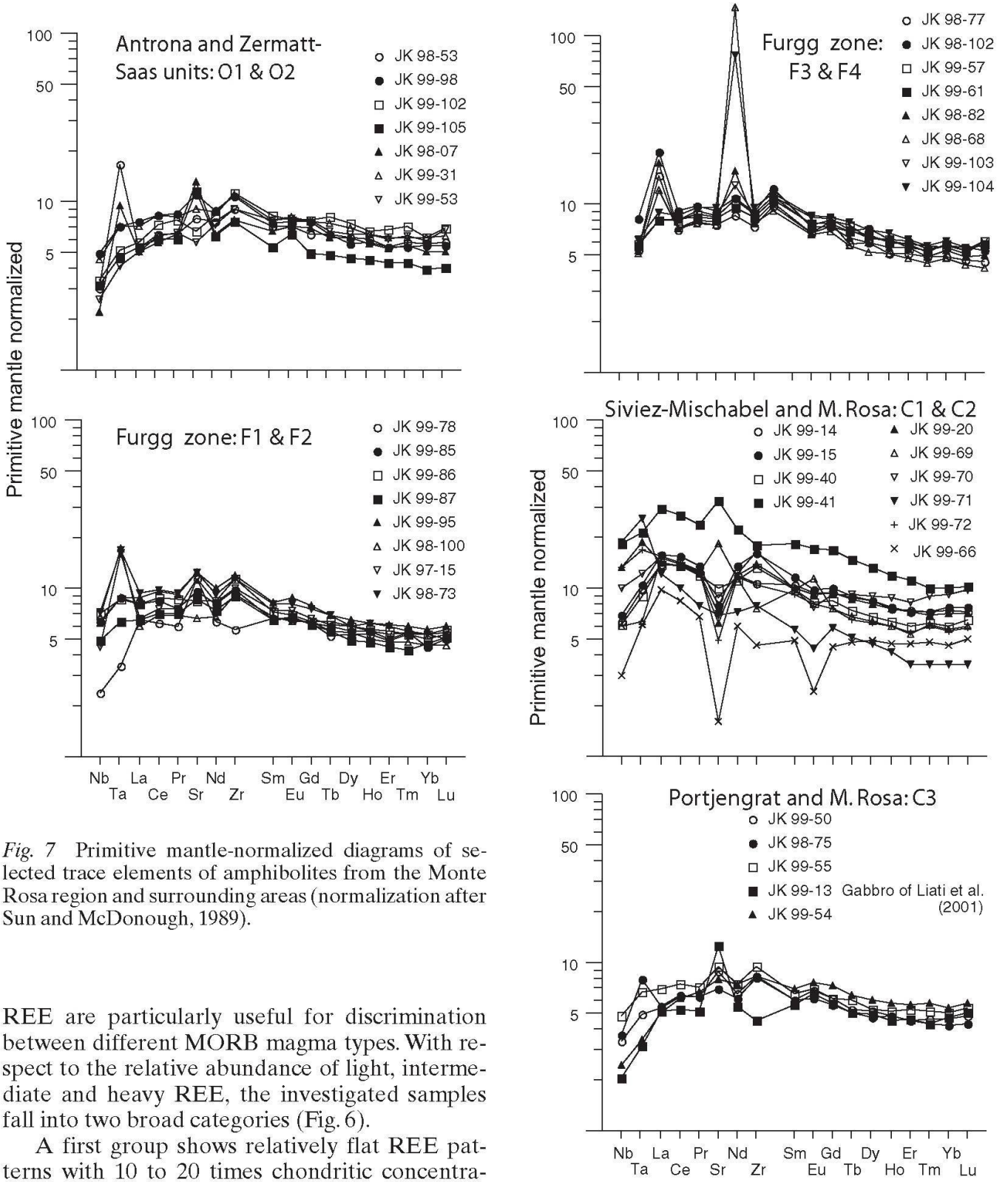

Fig. 7 Primitive mantle-normalized diagrams of selected trace elements of amphibolites from the Monte Rosa region and surrounding areas (normalization after Sun and McDonough, 1989).

REE are particularly useful for discrimination between different MORB magma types. With respect to the relative abundance of light, intermediate and heavy REE, the investigated samples fall into two broad categories (Fig. 6).

A first group shows relatively flat REE patterns with 10 to 20 times chondritic concentrations, typical for T-type MORB, with (Ce/Yb) between 1.00 and 1.76 (Table 2). This group includes all samples from the two ophiolitic units (O1 and O2), all samples from the Furgg zone (F1–F4) and the samples of group C3 (Fig. 6). Primitive mantle-normalized trace element patterns (Fig. 7; after Sun and MacDonough, 1989) indicate a consistent positive Zr anomaly, with the exception of two samples, which probably represent former gabbro cumulates (see below). Such a trace element pattern is not uncommon in basalts and is a characteristic feature of low-degree melts generated in the spinel peridotite field (e.g. Casey, 1997). Sr (and Rb, which is not shown) is highly variable and may reflect alteration processes related to the breakdown of plagioclase.

A second group of samples comprises dykes and sills from the Siviez-Mischabel basement unit (C1) and isolated boudins found within the southwestern part of the Monte Rosa basement and

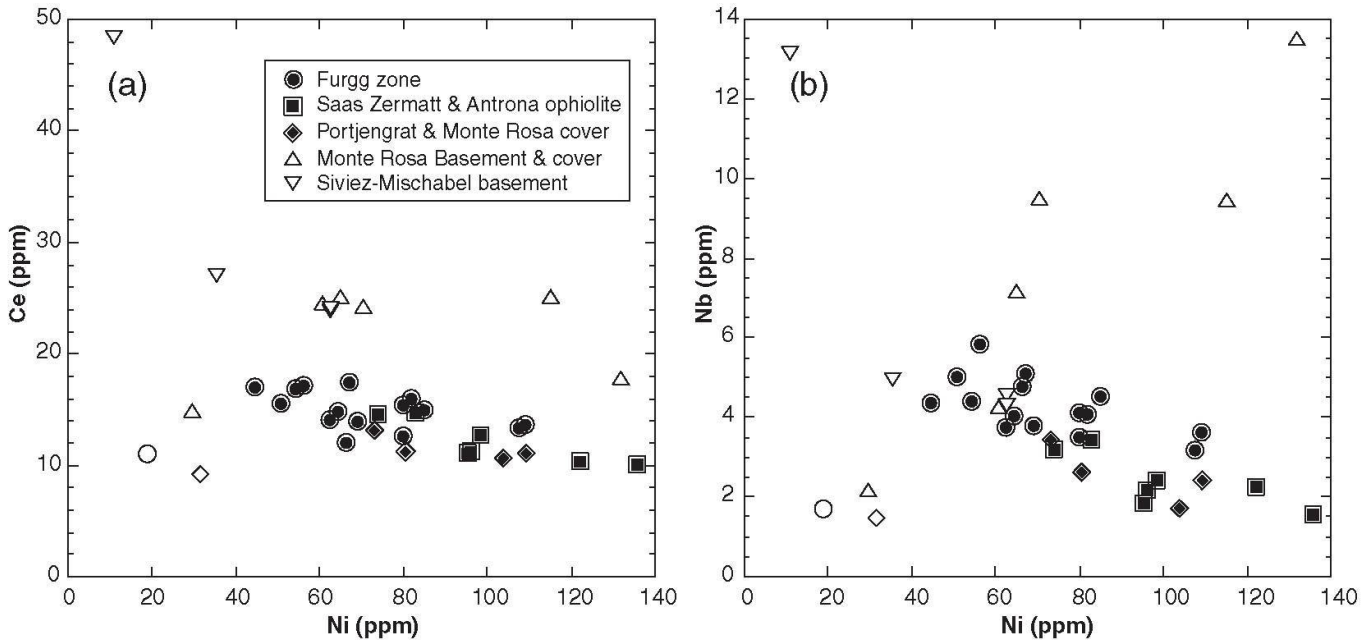

Fig. 8 (a) and (b). Compatible (Ni) versus incompatible element (Nb, Ce) plots. All samples (filled symbols) from the Furgg zone (except one, open circle), the Zermatt-Saas and Antrona ophiolitic units and the Portjengrat unit (except one, open diamond) indicate a coherent chemical trend with decreasing Ni and increasing incompatible elements (Ce, Nb). Open symbols show either low incompatible elements at low Ni content or high incompatible element content at variable Ni content (all samples from the Monte Rosa basement, and the Siviez-Mischabel nappe). These samples are probably not metabasalts but gabbro cumulates or gabbros with high proportions of trapped interstitial liquid or (in the case of the Siviez Mischabel nappe) metabasalts with a source enriched in incompatible elements.

cover (C2). These samples have highly variable REE patterns and slopes (Fig. 6). The compatible/ incompatible element ratios (Fig. 8) are different from those of the first group. As can be seen from Fig. 8, the C1 and C2 samples show different Ce/ Ni ratios and highly variable Nb contents. These features indicate that the C1 and C2 samples have a different origin than all the other samples.

6. Discussion and conclusions

6.1. Gabbro or basaltic precursors of the amphibolites?

It is often difficult to decide from whole rock analyses of amphibolites whether they were derived from basaltic or gabbroic precursor rocks. This problem is particularly difficult to tackle if the metamorphosed mafic rocks are differentiated, because Fe–Ti-oxide gabbros are often fine-grained and resemble metamorphosed basalts. Compatible element (Ni) versus incompatible elements (Ce, Nb) covariation trends may provide a chemical criterion for the distinction between different protoliths (see Fig. 8). If samples represent a single suite of crystallized liquids (e.g. basaltic rocks), smooth negative correlations between compatible and incompatible elements are expected. As can be seen from Fig. 8, all samples from the ophiolites, the Furgg zone (with one exception) and the Portjengrat unit (with one exception) show a smooth increase of incompatible Ce and Nb with decreasing Ni content. The samples falling off the trend most probably represent cumulates. These samples are not further considered in the discussion[1].

Compared to the samples from the ophiolitic units, the Furgg zone and the Portjengrat unit, the samples from the Siviez-Mischabel basement (C1) and the southwestern Monte Rosa nappe (C2) exhibit generally higher LREE contents at comparable Ni (Fig. 8) and REE spectra with higher LREE/ HREE ratios (Fig. 6). In addition, in the C2 group Nb is highly variable, which probably reflects different proportions of Fe–Ti oxides

[1] U–Pb dating of zircons from sample 99-13 (Monte Rosa cover) yielded a Paleozoic age (Liati et al., 2001), which was interpreted to represent the time of crystallization of the igneous (gabbroic?) protolith by these authors. However, the chemistry of this sample (Figs. 6, 8) is indicative of a cumulate precursor, and hence the sample is not representative of the suite of amphibolites in Furgg zone (group F1–F4), Portjengrat unit and northern Monte Rosa nappe (group C3). Since we do not regard the sample as part of the same magmatic suite, its Paleozoic age is not considered as representative of the other samples.

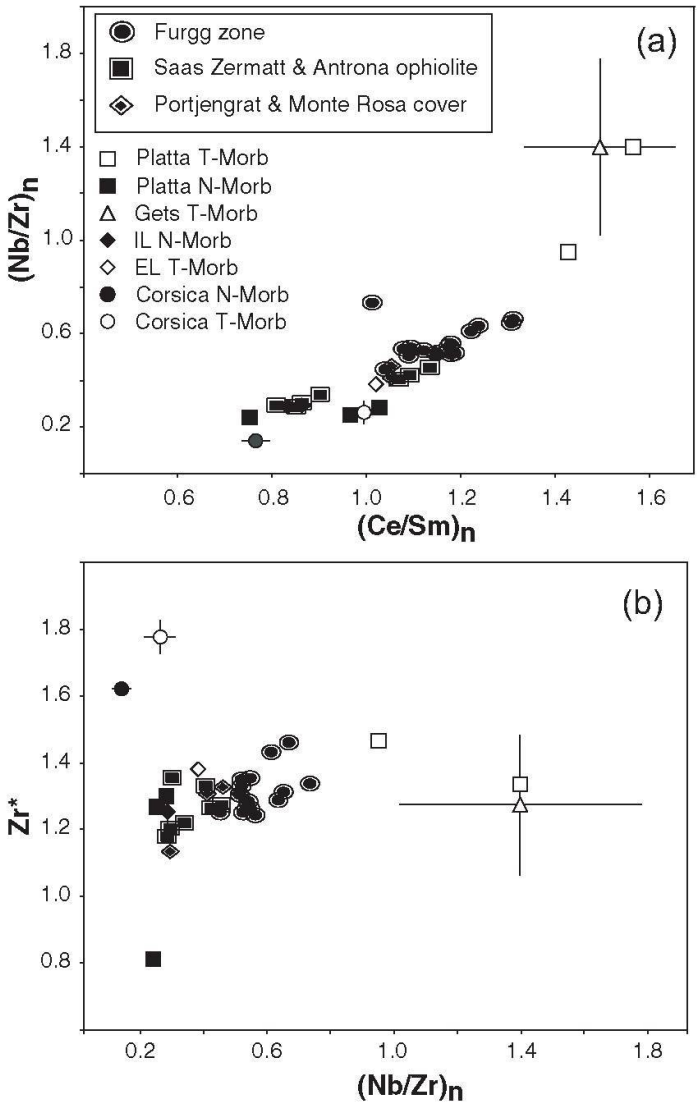

Fig. 9 Incompatible element ratio plots for metabasalts from the Furgg zone and adjacent areas, and comparison with basalts from other Piemont-Ligurian ophiolites. Only samples with filled symbols from Fig. 8 are plotted here. (a) $(Nb/Zr)_n$ vs. $(Ce/Sm)_n$ plot. High values for T-MORBs from the Gets and Platta nappe indicate an enriched mantle source, whereas the lower values for the N-MORBs from the Platta nappe, Ligurides and Corsica are similar to those of present-day N-MORBs. The samples from the Furgg zone are mostly T-MORB, while some samples from the Zermatt-Saas and Antrona ophiolitic units are approaching N-MORB. (b) Zr* $(Zr_n/((Sm_n+Nd_n)/2))$ vs. $(Nb/Zr)_n$ plot. Zr* is sensitive to changes in the degree of partial melting producing the basalts, whereas $(Nb/Zr)_n$ is characteristic of the source of melting. All data from the Furgg zone and adjacent areas indicate relatively low degrees of partial melting. Data sources (averages, thin lines indicate 2σ standard deviation of the mean): Gets nappe: Bill et al. (2000); Platta nappe: Desmurs et al. (2002); Internal and External Ligurides: Rampone et al. (1998); Corsica: Saccani et al. (2000).

in these samples. The smooth REE spectra from the Siviez-Mischabel basement (C1) may indicate enriched MORB (e.g. Bill et al., 2000) derived from a source with initially high incompatible element content. The samples from the southwestern Monte Rosa nappe (C2) do not show any systematics with respect to incompatible elements (Fig. 8). In addition, field relations indicate a possible Paleozoic origin for some of the amphibolites from the southwestern Monte Rosa nappe. This is why we think that the C1 and C2 amphibolites cannot be directly compared with the amphibolites from the ophiolites, the Furgg zone and the Portjengrat unit.

6.2. Possible sources of the MORB magmatism in the Furgg zone, the Portjengrat unit and adjacent ophiolitic units

In Figure 9a, the Nb_n/Zr_n and the Ce_n/Sm_n ratios of samples from the Furgg zone, the Portjengrat unit, the Antrona ophiolites and the Zermatt-Saas ophiolites are plotted and compared to basalts from Piemont-Ligurian ophiolites from outside the study area. The Ce_n/Sm_n and the Nb_n/Zr_n ratios of the Antrona and Zermatt-Saas ophiolites cluster in two different groups, one with $Ce_n/Sm_n < 1$ and $Nb_n/Zr_n < 0.4$, and one with $Ce_n/Sm_n > 1$ and $Nb_n/Zr_n > 0.4$, respectively (Fig. 9 a). The latter are very similar to the Furgg zone metabasalts and are intermediate between T-MORB from the Gets and upper Platta nappe, and T-MORB from the external Ligurides and Corsica (Fig. 9b). This suggests that the Furgg zone metabasalts are T-MORB from a single homogenous magma source while in the metabasalts from the adjacent ophiolitic units the source was more heterogeneous, producing basalts of T- to N-MORB composition. All metabasalts from the Furgg zone and from the Antrona and Zermatt-Saas ophiolites show a positive anomaly in Zr (Zr*). This probably indicates a low degree of melting in the spinel field (Casey, 1997). The Zr* decreases from T- to N-MORB in Corsica and the Ligurides. This indicates that they are the products of variable degrees of partial melting (higher for N- than T-

MORB). Taken together, these data show that partial melting of a slightly enriched (lithospheric?) mantle source led to the formation of the metabasalts from the Furgg zone (group F1–F4) and Portjengrat unit (group C3), whereas partial melting of a more depleted mantle source accounted for the formation of the metabasalts of the ophiolitic units (group O 1 and O2).

6.3. Tectonic implications of the geochemical data

The geochemical data discussed above suggest that the abundant small metabasaltic boudins of the Furgg zone (group F1–F4) are T-MORB type intrusives that were derived from a slightly enriched (lithospheric?) and single cogenetic magma suite. In this respect they differ from the ophiolitic units that exhibit a tendency towards a more depleted, T- to N-MORB type and towards a more heterogeneous magma source. If the Furgg zone metabasalts were derived from ophiolitic units, one would expect a complete overlap of the chemistry of the Furgg zone metabasalts with that of the metabasalts from the ophiolitic units. This is, however, not supported by our data (Figs. 8 and 9). Furthermore, the Zr, Y, V, and Ti interelement correlations are significantly higher in the Furgg zone metabasalts than in the mafic rocks from the ophiolitic units. This excludes the possibility that the Furgg zone metabasalts were derived through tectonic incorporation of adjacent ophiolitic components. In summary, these data indicate that the Furgg zone cannot be interpreted as an ophiolitic mélange, as proposed by Froitzheim (2001).

Given the geochemical similarities of the metabasaltic boudins of the Furgg zone with those of the Portjengrat unit (group C3), the main difference between the two units seems to be the continuous increase in strain intensity towards the Furgg zone. Since the Portjengrat unit is undoubtedly a fragment of continental upper crust, the Furgg zone may conclusively be interpreted as an intracontinental shear zone that overprints both Portjengrat unit and adjacent Monte Rosa nappe. This is consistent with structural evidence indicating that the Monte Rosa nappe and the Portjengrat-Stockhorn units were originally connected to form a single Portjengrat – Stockhorn – Monte Rosa continental fragment, separating the Antrona ophiolites from the Zermatt-Saas ophiolites (Keller and Schmid, 2001; Kramer, 2002). This is again in marked contrast to the model proposed by Froitzheim (2001), who considers the Furgg zone, together with the Antrona ophiolitic unit, as representing North Penninic oceanic crust, which separates the Briançonnais microcontinent (the Portjengrat-Stockhorn unit) from the European plate (the Monte Rosa nappe). However, the geochemical data presented above do not exclude the possibility that the Antrona and Zermatt-Saas units were an originally continuous unit forming part of the Piemont-Ligurian ocean, as was proposed by Escher et al. (1997).

The different geochemical signatures of the metabasaltic boudins from the intensely strained Monte Rosa cover and basement of the southwestern Monte Rosa nappe (ISMR, group C2) preclude a direct correlation with the Furgg zone, as was proposed by Dal Piaz (1966). Furthermore, their derivation from the Zermatt-Saas ophiolitic unit can also be excluded on geochemical arguments. Hence, the chemical data presented in this study do not support the idea that the ISMR represents the prolongation of the Furgg zone in terms of an ophiolitic mélange (Froitzheim, 2001). On the other hand, larger mappable ophiolitic slivers containing ultramafic rocks, which are surrounded by the Furgg zone, do exist. However, they demonstrably are either isoclinal D3 fold cores of the Zermatt-Saas unit (at Gornergrat) or fold cores of the Antrona unit (in the Monte della Preja region) that were fragmented during D3 overprint (Kramer, 2002) and that are not regarded as part of the Furgg zone (Keller and Schmid, 2001; Kramer, 2002).

6.4. Paleogeographic implications of the geochemical data

Based on the geochemistry of the metabasalts, two stages of mafic magmatism are inferred. An early stage is recorded by the samples of groups C1 and C2. The amphibolite boudins of group C2 are embedded in the basement of the southwestern Monte Rosa nappe (ISMR), as well as in garnet micaschists of its supposedly Permo-Triassic meta-sedimentary cover. The boudins are parallel to the foliation of the basement rocks, which is, at least in part, defined by pre-Alpine sillimanite (Dal Piaz, 1966). Hence, Dal Piaz concluded, that foliation and embedded boudins are Paleozoic in age. This view is corroborated by the observation of amphibolite boudins, which are intruded by granites of probably Permian (or Late Carboniferous) age (Kramer, 2002). Late Carboniferous to Permian igneous activity, producing MORB-type and also more differentiated magmas has been described from several regions in the Alps (e.g. von Raumer et al., 1990). A pre-Triassic age is also likely for the amphibolites of group C1 from the Siviez-Mischabel nappe, which were collected within the basement only.

A later, presumably post-Triassic age is proposed for all T-type MOR basalts. The main reasoning is that some of the metabasalts of groups C3 (Portjengrat and Stockhorn units) and F4 (parts of the Furgg zone) intruded Triassic metaarkoses and/or marbles (Jaboyedoff et al., 1996; Kramer, 2002). Our geochemical data and field relations suggest that this post-Triassic MORB-type magmatism affected pericontinental as well as oceanic units. This has recently been described from other ocean-continent transition zones in the Eastern Central Alps (e.g. Puschnig, 2000; Desmurs et al., 2002) and in the Gets nappe (Bill et al., 2000). However, in none of these regions were comparable volume proportions of mafic rocks found within continental upper crustal basement, including its Triassic cover.

The question whether the Furgg zone magmatism was linked in space and time with the magmatism in the ophiolitic Antrona or with that of the Zermatt-Saas unit cannot be answered unequivocally with the existing geochemical data alone. In case of the existence of only one single oceanic basin in the working area, as proposed by Escher et al. (1997), all ophiolitic units would have belonged to the Piemont-Ligurian ocean. According to this tectonic model, this single oceanic suture derived from South Penninic oceanic crust would separate Austroalpine units from the Briançonnais microcontinent, the southern margin of which would be represented in our working area.

In case of the existence of two oceanic basins in the working area, the Antrona and Zermatt-Saas units would have been part of the Valais and Piemont-Ligurian oceans, respectively (e.g. Keller and Schmid, 2001). Those metabasalts that pertained to the Valaisan ocean, would be Late Jurassic or younger in age. The fact that the adjacent Portjengrat unit and Furgg zone were intruded by dykes and sills with T- to N-MORB compositions similar to the ophiolites suggests that both units may have been derived from the same distal continental margin within the Briançonnais, that was stacked between the Valaisan and Piemont-Ligurian oceanic sutures. According to this scenario the Portjengrat-Stockhorn-Monte Rosa continental fragment (including the Furgg zone) represents the eclogitic part of the Briançonnais microcontinent, as proposed by Keller and Schmid (2001) and Kramer (2002).

Structural studies indicate that the distal margin of the Briançonnais, represented by the Portjengrat unit and the Furgg zone, may have been located adjacent to the more external Valaisan oceanic basin (Keller and Schmid, 2001). In this context it is interesting to note that T-type MORB dykes have neither been reported from the sedimentary cover of the Siviez-Mischabel nappe (internal Briançonnais), nor from the southwestern part of the Monte Rosa nappe (most internal Briançonnais situated directly adjacent to undisputed Piemont-Liguran ophiolites, i.e. the Zermatt-Saas unit; see Figs. 1 and 2). Together with the fact that ophiolitic imbricates derived from the Antrona unit (Valaisan according to Keller and Schmid, 2001) can be found in the Furgg zone, these structural and field arguments may indicate that the basaltic intrusions into distal continental margin units occurred in the context of Late Jurassic to Early Cretaceous opening of the Valais ocean.

Notwithstanding the different paleotectonic interpretations, an important finding of this study is that T-type MOR basalts are not only found in ophiolitic units but also in (thinned) distal continental margin units. The volume of mafic rocks intruding the Briançonnais distal continental margin adjacent to the Valais ocean or, alternatively, to the Piemont-Ligurian ocean, is distinctly higher than the volume of mafic rocks found in the Adriatic distal continental margin (e.g. Puschnig, 2000; Desmurs et al., 2002). This 'asymmetry' in the distribution of mafic rocks along continental margins is consistent with asymmetric low angle detachment faulting during the latest stages of rifting. The finding of T-MOR basalts intruding distal parts of the continental crust is similar to the evolution of the Red Sea rifting system (e.g. Voggenreiter et al., 1988).

Acknowledgements

The authors gratefully acknowledge the contributions of all the members of the Basel, Bonn and Mainz "Monte Rosa group" (Nikolaus Froitzheim, Ronan Le Bayon, Katharina Dubach, Christiane Rössler, Lukas Keller, Andreas Weber, Corinne Bacher, Lukas Baumgartner, Sabine Pawlig). Furthermore, we benefitted from discussions with and/or reviews from Hans-Rudolf Pfeifer, Philippe Monjoie, Dieter Gebauer, and Martin Engi.
J. Kramer acknowledges support from the Werenfels-Fonds, Freiwillige Akademische Gesellschaft, Basel. S. Schmid acknowledges support from NF-projects Nr. 20-61814.00 and 2000-068020/1, initiated by the late Martin Frey. The authors are grateful for Martin's initiative and support during the initial stages of this study.

References

Amato, J.M., Johnson, C.M., Baumgartner, L.P. and Beard, B.L. (1999): Rapid exhumation of the Zermatt-Saas ophiolite deduced from high-precision Sm–Nd and Rb–Sr geochronology. *Earth Planet. Sci. Lett.* **171**, 425–438.

Bacher, C. (2002): Strukturen und Metamorphose in der Furggzone (Furggtal bei Saas Almagell, Wallis). Unpubl. diploma thesis, University of Basel, 83 pp.

Barnicoat, A.C. and Fry, N. (1986): High-pressure metamorphism of the Zermatt-Saas ophiolite zone, Switzerland. *J. Geol. Soc. London* **143**, 607–618.

Barnicoat, A.C., Rex, D.C., Guise, P.G. and Cliff, R.A. (1995): The timing of and nature of greenschist facies deformation and metamorphism in the upper Pennine Alps. *Tectonics* **14**, 279–293.

Bearth, P. (1945): Ueber das Verhältnis von Kristallisation und Bewegung in der Monte Rosa-Bernhard-(Mischabel)-Decke. *Schweiz. Mineral. Petrog. Mitt.* **25**, 537–538.

Bearth, P. (1952): Geologie und Petrographie des Monte Rosa. *Beitr. Geol. Karte Schweiz (Neue Folge)* **96**, 1–94.

Bearth, P. (1953a): Blatt Zermatt, Geologischer Atlas der Schweiz, Nr. 29. 1:25'000. Basel, Schweiz. Geol. Kommission.

Bearth, P. (1953b): Erläuterungen Blatt Zermatt, Geologischer Atlas der Schweiz. Nr. 29. 1:25'000. Basel, Schweiz. Geol. Kommission.

Bearth, P. (1954a): Blatt Monte Moro, Geologischer Atlas der Schweiz, Nr. 30. 1:25'000. Basel, Schweiz. Geol. Kommission.

Bearth, P. (1954b): Blatt Saas, Geologischer Atlas der Schweiz, Nr. 31. 1:25'000. Basel, Schweiz. Geol. Kommission.

Bearth, P. (1956): Geologische Beobachtungen im Grenzgebiet der lepontinischen und penninischen Alpen. *Eclogae geol. Helv.* **49**, 279–290.

Bearth, P. (1957): Erläuterungen Blatt Saas und Monte Moro, Geologischer Atlas der Schweiz. Nr. 30, 31. Basel, Schweiz. Geol. Kommission.

Bearth, P. (1976): Zur Gliederung der Bündnerschiefer in der Region von Zermatt. *Eclogae geol. Helv.* **69**, 149–161.

Bearth, P. and Schwander, H. (1981): The post-Triassic sediments of the ophiolite zone Zermatt-Saas Fee and the associated manganese mineralizations. *Eclogae geol. Helv.* **74**, 189–205.

Bearth, P. and Stern, W. (1971): Zum Chemismus der Eklogite und Glaukophanite von Zermatt. *Schweiz. Mineral. Petrogr. Mitt.* 51, 349–359.

Bearth, P. and Stern, W. (1979): Zur Geochemie von Metapillows der Region Zermatt-Saas. *Schweiz. Mineral. Petrogr. Mitt.* **59**, 349–373.

Beccaluva, L., Dal Piaz, G.V. and Macciotta, G. (1984): Transitional to normal MORB affinities in ophiolitic metabasites from Zermatt-Saas, Combin and Antrona units, Western Alps. *Geol. Mijnbouw* **63**, 165–177.

Bill, M., Nägler, T.F. and Masson, H. (2000): Geochemistry, Sm–Nd and Sr isotopes of mafic rocks from the earliest oceanic crust of Alpine Tethys. *Schweiz. Mineral. Petrogr. Mitt.* **80**, *131–145.*

Boynton, W.V. (1984): Cosmochemistry of the rare earth elements: meteorite studies. In: Henderson, P. (ed.): Developments in Geochemistry 2 – Rare Earth Element Geochemistry. Elsevier, Amsterdam, 63–114.

Carrupt, E. and Schlup, M. (1998): Métamorphisme et tectonique du versant sud du Val Bognanco (Pennique, Alpes italiennes). *Bull. Soc. Vaud. Sci. Nat.* **86**, 29–59.

Casey, J.F. (1997): Comparison of major- and trace element geochemistry of abyssal peridotites and mafic plutonic rocks with basalts from the MARK region of the Mid-Atlantic Ridge. *Proc. Ocean. Drill. Prog. Sci. Res.* **153**, 181–241.

Colombi, A. (1989): Métamorphisme et géochimie des roches mafiques des Alpes ouest-centrales (géoprofil Viège-Domodossola-Locarno). *Mém. Géol.* **4**. Imprivite S.A., Lausanne, 216 pp.

Cullers, R.L. and Graf, J.L. (1984): Rare earth elements in igneous rocks of the continental crust: predominantly basic and ultrabasic rocks. In: Henderson, P. (ed.): Developments in Geochemistry 2 – Rare Earth Element Geochemistry. Elsevier, Amsterdam, 237–274.

Dal Piaz, G.V. (1964): Il cristallino antico del versante meridionale del Monte Rosa paraderivati a prevalente metamorphismo alpino. *Rendiconti Soc. Min. Italiana Anno XX*, 101–135; 4 Tav.

Dal Piaz, G.V. (1966): Gneiss ghiandoni, marmi ed anfiboliti antiche del ricoprimento Monte Rosa nell'alta Valle d'Ayas. *Boll. Soc. Geol. Italiana* **85**, 103–132.

Dal Piaz, G.V. (1971): Nuovi ritrovamenti di cianite alpina nel Cristallino antico del Monte Rosa. *Rend. Soc. Italiana Min. Petrol.* **27**, 437–477.

Dal Piaz, G.V. (2001): Geology of the Monte Rosa massif: historical review and personal comments. *Schweiz. Mineral. Petrogr. Mitt.* **81**, 275–303.

Desmurs, L., Müntener, O. and Manatschal, G. (2002): Onset of magmatic accretion within a magma-poor rifted margin: A case study from the Platta ocean-continent transition, Eastern Switzerland. *Contrib. Mineral. Petrol.* **144**, 365–382.

Dostal, J. and Capedri, S. (1979): Rare earth elements in high-grade metamorphic rocks from the Western Alps. *Lithos* **12**, 41–49.

Dubach, K. (1998): Die Grenzzone von Portjengrat-Einheit und Siviez-Mischabel-Decke im Almagellertal, Wallis. Unpubl. diploma thesis, University of Basel, 61 pp.

Eisele, J., Geiger, S. and Rahn, M. (1997): Chemical characterization of metabasites from the Turtmann Valley (Valais, Switzerland): implications for their protoliths and geotectonic origin. *Schweiz. Mineral. Petrogr. Mitt.* **77**, 403–417.

Engi, M., Scherrer, N.C. and Burri, T. (2001): Metamorphic evolution of pelitic rocks of the Monte Rosa nappe: Constraints from petrology and single grain monazite age data. *Schweiz. Mineral. Petrogr. Mitt.* **81**, 305–328.

Escher, A., Hunziker, J.-C., Marthaler, M., Masson, H., Sartori, M. and Steck, A. (1997): Geologic framework and structural evolution of the western Swiss-Italian Alps. In: Pfiffner, O.A., Lehner, P., Heitzmann, P., Müller, S. and Steck, A. (eds.): Deep structure of the Swiss Alps: Results from NRP 20. Birkhäuser, Basel, 205–221.

Escher, A., Masson, H. and Steck, A. (1988): Coupes géologiques des Alpes occidentales suisses. Mém. Géol. Lausanne, *Rapp. géol. serv. hydrol. géol. natl.* **2**, 1–11, incl. 1 map, 2 tables, 1 plate.

Escher, A. and Sartori, M. (1991): The geology of the Zermatt-Gornergrat area. NFP 20 Bull. 9, 5–11.

Frey, M., Hunziker, J.C., O'Neil, J.R. and Schwander, H.W. (1976): Equilibrium-disequilibrium relations in the Monte Rosa Granite, Western Alps; petrological, Rb–Sr and stable isotope data. *Contrib. Mineral. Petrol.* **55**, 147–179.

Froitzheim, N. (2001): Origin of the Monte Rosa nappe in the Pennine Alps – A new working hypothesis. *Geol. Soc. Am. Bull.* **113**, 604–614.

Gebauer, D. (1999): Alpine geochronology of the Central and Western Alps: new constraints for a complex geodynamic evolution. *Schweiz. Mineral. Petrogr. Mitt.* **79**, 191–208.

Gelinas, L., Mellinger, M. and Trudel, P. (1982): Archaean mafic metavolcanics from the Rouyn-Noranda district, Abitibi greenstone belt, Quebec. 1. Mobility of the major elements. *Canad. J. Earth Sci.* **19**, 2258–2275.

Grauch, R.I. (1989): Rare earth elements in metamorphic rocks. In: Lipin, B.R. and McKay, G.A. (eds.): Geochemistry and mineralogy of rare earth ele-

ments. 21. Mineralogical Society of America, Washington D.C., 147–167.
Henderson, P. (1984): General geochemical properties and abundances of the rare earth elements. In: Henderson, P. (ed.): Developments in Geochemistry 2 – Rare Earth Element Geochemistry. Elsevier, Amsterdam Oxford New York Tokyo, 1–32.
Huang, T.-K. (1935a): Carte géologique de la région Weissmies-Portjengrat (Valais). 1:25'000. Basel, Schweiz. Geol. Kommission.
Huang, T.-K. (1935b): Etude géologique de la région Weissmies-Portjengrat (Valais). *Bull. Soc. Neuchat. Sci. Nat.* **60**, 3–76.
Humphris, S.E. (1984): The mobility of the rare earth elements in the crust. In: Henderson, P. (ed.): Developments in Geochemistry 2 – Rare Earth Element Geochemistry. Elsevier, Amsterdam, 317–342.
Hunziker, J.C. (1970): Polymetamorphism in the Monte Rosa, Western Alps. *Eclogae geol. Helv.* **63**, 151–161.
Jaboyedoff, M., Béglé, P. and Lobrinus, S. (1996): Stratigraphie et évolution structurale de la zone de Furgg, au front de la nappe du Mont-Rose. *Bull. Soc. Vaud. Sci. Nat.* **84**, 191–210.
Keller, L. (2000): Kinematik der duktilen Scherung an der Front der Monte Rosa Decke (Val Loranco, Italien). Unpubl. diploma thesis, University of Basel, 90 pp.
Keller, L. and Schmid, S.M. (2001): On the kinematics of shearing near the top of the Monte Rosa nappe and the nature of the Furgg zone in the Val Loranco (Antrona valley, N. Italy): tectono-metamorphic and paleogeographical consequences. *Schweiz. Mineral. Petrogr. Mitt.* **81**, 347–367.
Klein, J.A. (1978): Post-nappe folding southeast of the Mischabelrückfalte (Pennine Alps) and some aspects of the associated metamorphism. *Leidse geol. Medel.* **51**, 233–312.
Kramer, J. (2002): Structural evolution of the Penninic units in the Monte Rosa region (Swiss and Italian Alps). PhD thesis No. 24, University of Basel, 147 pp, 2 maps, 2 encl.
Le Bas, M.J., Le Maître, R.W., Streckeisen, A. and Zanettin, B. (1986): A chemical classification of volcanic rocks based on the total alkali-silica diagram. *J. Petrol.* **27**, 745–750.
Le Bayon, R., Schmid, S.M. and De Capitani, C. (2001): The metamorphic evolution of the Monte Rosa nappe and its relation to exhumation by fore- and back-thrusting in the Western Alps. *Geol. Paläont. Mitt. Innsbruck* **25**, 132–133.
Liati, A., Gebauer, D., Froitzheim, N. and Fanning, M. (2001): U–Pb SHRIMP geochronology of an amphibolitized eclogite and an orthogneiss from the Furgg zone (Western Alps) and implications for its geodynamic evolution. *Schweiz. Mineral. Petrogr. Mitt.* **81**, 379–393.
MacGeehan, P.J. and MacLean, W.H. (1980): An Archaean sub-seafloor geothermal system, 'calc-alkali' trends, and massive sulphide genesis. *Nature* **286**, 767–771.
Markley, M.J., Teyssier, C., Cosca, M.A., Caby, R., Hunziker, J.C. and Sartori, M. (1998): Alpine deformation and $^{40}Ar/^{39}Ar$ geochronology of synkinematic white mica in the Siviez-Mischabel nappe, Western Pennine Alps, Switzerland. *Tectonics* **17**, 407–425.
Marthaler, M. (1981): Découverte de foraminifères planctoniques dans les "schistes lustrés" de la pointe de Tourtemagne (Valais). *Bull. Soc. Vaud. Sci. Nat.* **75**, 171–178.
Marthaler, M. (1984): Géologie des unités penniniques entre le Val d'Anniviers et le Val de Tourtemagne (Valais, Suisse). *Eclogae geol. Helv.* **77**, 395–448.
Mattirolo, E., Novarese, V., Franchi, S. and Stella, A. (1912): Foglio Monte Rosa, Carta Geologica d' Italia. No. 29. 1:100 000. Novara, Serv. Geol. Italia.
Milnes, A.G., Greller, M. and Müller, R. (1981): Sequence and style of major post-nappe structures, Simplon-Pennine Alps. *J. Struct. Geol.* **3/4**, 411–420.
Mottl, M.J. (1983): Metabasalts, axial hot springs, and the structure of hydrothermal systems at mid-ocean ridges. *Geol. Soc. Am. Bull.* **94**, 161–180.
Müller, C. (1989): Albitisation of the Zermatt area, Western Alps. PhD thesis, University of Basel, 285 pp.
Pearce, J.A. (1976): Statistical analysis of major element patterns in basalts. *J. Petrol.* **17**, 15–43.
Pearce, J.A. (1982): Trace element characteristics of lavas from destructive plate boundaries. In: Thorpe, R.S. (ed.): Andesites – Orogenic andesites and related rocks. John Wiley and Sons, Chichester, 525–548.
Pfeifer, H.R., Colombi, A. and Ganguin, J. (1989): Zermatt-Saas and Antrona Zone: A petrographic and geochemical comparison of polyphase metamorphic ophiolites of the West-Central Alps. Schweiz. *Mineral. Petrogr. Mitt.* **69**, 217–236.
Puschnig, A.R. (2000): The oceanic Forno Unit (Rhetic Alps). *Eclogae Geol. Helv.* **93**, 103–124
Rampone, E., Hofmann, A.W. and Raczek, I. (1998: Isotopic contrasts within the Internal Liguride Ophiolite (N. Italy): the lack of a genetic mantle-crust link. *Earth Planet. Sci. Lett.* **163**, 175–189.
Reinecke, T. (1991): Very-high-pressure metamorphism and uplift of coesite-bearing metasediments from the Zermatt-Saas zone, Western Alps. *Eur. J. Mineral.* **3**, 7–17.
Reinecke, T. (1998): Prograde high- to ultrahigh-pressure metamorphism and exhumation of oceanic sediments at Lago di Cignana, Zermatt-Saas Zone, western Alps. *Lithos* **42**, 147–189.
Rollinson, H.R. (1993): Using geochemical data: evaluation, presentation, interpretation. Longman, Singapore, 352 pp.
Rössler, C. (2000): Transport und Faltung in der Furggzone und in den angrenzenden Einheiten (südliches Saastal, Wallis, Schweiz). Unpubl. diploma thesis, University of Basel, 74 pp.
Rubatto, D. and Gebauer, D. (1999): Eo/Oligocene (35 Ma) high-pressure metamorphism in the Gornergrat Zone (Monte Rosa, Western Alps): implications for paleogeography. *Schweiz. Mineral. Petrogr. Mitt.* **79**, 353–362.
Saccani, E., Padoa, E. and Tassinari, R. (2000): Preliminary data on the Pineto gabbroic massif and Nebbio basalts: Progress toward the geochemical characterization of Alpine Corsica ophiolites. *Ofioliti* **25**, 75–85.
Sartori, M. (1987): Structure de la zone du Combin entre les Diablons et Zermatt (Valais). *Eclogae geol. Helv.* **80**, 789–814.
Sartori, M. (1990): L'unité du Barrhorn (Zone pennique, Valais, Suisse). PhD thesis, University of Lausanne, 156 pp.
Saunders, A.D. (1984): The rare earth element characteristics of igneous rocks from the ocean basins. In: Henderson, P. (ed.): Developments in Geochemistry 2 – Rare Earth Element Geochemistry. Elsevier, Amsterdam Oxford New York Tokyo, 205–236.
Saunders, A.D. and Tearney, J. (1984): Geochemical characteristics of basaltic volcanism within back-arc basins. In: Kohelaar, B.P. and Howells, M.F. (eds.): Marginal basin geology. *Geol. Soc. London Spec. Publ.* **16**., 59–76.
Schilling, J.-G., Zajac, M., Evans, R., Johnston, T., White, W., Devine, J.D. and Kingsley, R. (1983): Petrologic

and geochemical variations along the Mid-Atlantic Ridge from 27°N to 73°N. *Am. J. Sci.* **283**, 510–586.
Schmid, S.M. and Kissling, E. (2000): The arc of the western Alps in the light of geophysical data on deep crustal structure. *Tectonics* **19**, 62–85.
Stampfli, G.M. and Marchant, R.H. (1997): Geodynamic evolution of the Tethyan margins of the Western Alps. In: Pfiffner, O.A. and others (eds.): Deep structure of the Swiss Alps: results of NRP 20. Birkhäuser, Basel, 223–239.
Steck, A., Epard, J.-L., Escher, A., Gouffon, Y. and Masson, H. (1999): Carte téctonique des Alpes de Suisse occidentale et des régiones avoisinantes. Feuille Monte Rosa, No. 47. 1:100'000. Bern, *Serv. hydrol. géol. nat.*
Sun, S.S. and McDonough, W.F. (1989): Chemical and isotopic systematics of oceanic basalts: implications for mantle composition and processes. In: Saunders, A.D. and Norry, M.J. (eds.): Magmatism in ocean basins. *Geol. Soc. London Spec. Publ.* **42**, 313–345.
Thélin, P., Sartori, M., Burri, M., Gouffon, Y. and Chessex, R. (1993): The Pre-Alpine Basement of the Briançonnais (Wallis, Switzerland). In: von Raumer, J.F. and Neubauer, F. (eds.): Pre-Mesozoic Geology in the Alps. Springer, Berlin, 297–315.
Thélin, P., Sartori, M., Lengeler, R. and Schaerer, J.P. (1990): Eclogites of Paleozoic or early Alpine age in the basement of the Penninic Siviez-Mischabel Nappe, Wallis, Switzerland. *Lithos* **25**, 71–88.
van der Klauw, S.N.G.C., Reinecke, T. and Stöckhert, B. (1997): Exhumation of ultrahigh-pressure metamorphic oceanic crust from Lago di Cignana, Piemontese zone, western Alps: the structural record in metabasites. *Lithos* **41**, 79–102.
Venturelli G., Thorpe R.S. and Potts P.J. (1981): Rare earth and trace element characteristics of ophiolitic metabasalts from the Alpine-Apennine belt. *Earth Planet. Sci. Lett.* **53**, 109–123.
von Raumer, J.F., Galetti, G., Pfeifer, H.R. and Oberhänsli, R. (1990): Amphibolites from Lake Emosson/Aiguilles Rouges, Switzerland: tholeiitic basalts of a Paleozoic continental rift zone. *Schweiz. Mineral. Petrogr. Mitt.* **70**, 419–435.
Weber, A. (2001): Zur strukturellen und metamorphen Entwicklung der Furgg-Zone und angrenzender Einheiten im südlichen Saastal, Wallis, Schweiz. Unpubl. diploma thesis, University of Bonn, 85 pp.
Wetzel, R. (1972): Zur Petrographie und Mineralogie der Furgg-Zone (Monte Rosa-Decke). *Schweiz. Mineral. Petrogr. Mitt.* **52**, 161–236.
Wood, D.A., Joron, J.-L. and Treuil, M. (1979): A re-appraisal of the use of trace elements to classify and discriminate between magma series erupted in different tectonic settings. *Earth Planet. Sci. Lett.* **45**, 326–336.

Received 12 July 2002
Accepted in revised form 14 July 2003
Editorial handling: M. Engi